SIMULATION OF FINITE MEMORY HOLD CIRCUITS

by

Barry Arthur Howarth, B. Eng., P. Eng.

A thesis submitted to the Faculty of Graduate Studies and Research in partial fulfilment of the requirements for the degree of Master of Engineering.

Electrical Engineering Department,
McGill University,
MONTREAL, P. Q.

April, 1962.

A C K N O W L E D G E M E N T S

The author wishes to thank Dr. T.J.F. Pavlasek for his supervision and guidance. He also acknowledges the advice and suggestions offered by members of the staff of the Computing Center and Professor S. Melamed of the Mathematics Department of McGill University.

Mr. I. Borissov took the photograph of the experimental facilities. The thesis was typed by Mrs. M. A. Howarth and Miss Jean Frost.

This research was financed by the National Research Council.

TABLE OF CONTENTS

A B S T R A C T

This study demonstrates that a finite-memory hold circuit is a sampled-data filter which performs mathematical operations on discrete signals by using finite difference techniques. Some alternate proofs to theorems pertaining to sampled-data systems are offered in addition to the derivation of a general expression for the transfer function of the hold circuit which restores sampled-data signals to an analog form. An analysis of the errors arising in such a restoration is presented.

A method of simulating such filters using operational amplifiers is suggested and the requirements which the various components in such a scheme must satisfy is investigated. The circuitry employed in such a system is described, including the design and performance of a direct-coupled diode switch, capable of high operating speeds which may be used for sampling and gating.

The experimental results obtained with a prototype simulation system are compared with z- transform predictions. Some applications of these sampled-data filters are suggested as areas for future research.

CHAPTER I

SAMPLED-DATA SYSTEMS

1.1 Introduction

Concerted interest in sampled-data systems began in the early 1940's in connection with radar control. The results of these early investigations were summarized by James et al.[1] Since then there has been great activity in the analysis of sampled-data systems as witnessed by the volume of literature published on this subject in the past decade.[2,3,4]

A sampled-data system differs from a continuous one in the form in which information signals are transmitted. In the continuous case the signal is available at all times, while in the sampled-data case it is only available at discrete instants in time and hence is applied discontinuously to the system. The use of a sampled-data system may be dictated by economic reasons or considerations of weight and size. Thus, in control systems where digital computers are employed in the control loop, the input and output to the computer must be in a discrete or sampled-data form. Similarly, in telemetering systems, it may be necessary to time-share a communication channel among several units, and thus the transmitted information is received in the form of sampled-data.

James et al.[1] presented an analysis of sampled or pulsed data systems which was based on specifying the weighting function for a linear filter with pulsed data. Their method has the disadvantage of great mathematical complexity, although there is mention of the now popular Z-transform method of analysis. MacColl[5] discussed sampled-data servomechanisms and made a preliminary approach to the Z-transform.

1.2 Frequency-Domain Analysis

Linvill[6] analysed sampled-data systems in conventional frequency domain terms. In particular, he showed that the sampling process produces higher-order frequencies which may be removed by appropriate filtering. He also showed that no frequency higher than half the sampling frequency will be recovered in demodulating the sampled-data. This is a well known result previously established by Shannon.[7]

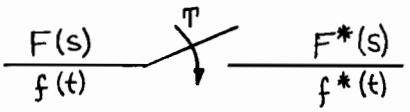

Figure 1.1

Schematic Representation of the Sampling Process

The sampling process is represented schematically in Figure 1.1 A commutater switch closes for an infinitesimally short time every T seconds, producing a sampled output $f^*(t)$ from the continuous input $f(t)$. It is assumed in the ensuing analysis that the output from the sampler consists of a train of impulses equally spaced in time and with areas equal to the value of $f(t)$ at the sampling instants. $F(s)$ is the Laplace Transform of $f(t)$ and $F^*(s)$ is the Laplace Transform of the sampled output.

Linville considered the sampling process to be amplitude modulation of an infinite pulse train by the input signal. If $\delta_T(t)$ represents an infinite train of unit impulses spaced T seconds apart, the sampling process may be represented mathematically by the expression:

$$f^*(t) = f(t) \times \delta_T(t) \qquad \ldots\ldots 1.1$$

The infinite pulse train may be expressed in the form of a complex Fourier Series:[6]

$$\delta_T(t) = \frac{1}{T} \sum_{k=-\infty}^{\infty} e^{jk\omega t} \qquad \ldots\ldots 1.2$$

where $T = 2\pi/\omega$ is the interval between sampling impulses.

If $F^*(\omega) = \int_{-\infty}^{\infty} f^*(t)e^{-j\omega t}\,dt$ is the Fourierc Transform of $f^*(t)$, then we may write:

$$F^*(\omega) = \int_{-\infty}^{\infty} f(t)\frac{1}{T_1}\sum_{k=-\infty}^{\infty} e^{jk\omega_1 t}\, e^{-j\omega t}\,dt \qquad \ldots. 1.3a$$

Assuming absolute convergence of the infinite series, and putting $k = -n$:

$$F^*(\omega) = \frac{1}{T_1}\sum_{n=-\infty}^{\infty}\int_{-\infty}^{\infty} f(t)\, e^{-j(\omega+n\omega_1)t}\,dt \qquad \ldots. 1.3b$$

$$= \frac{1}{T_1}\sum_{n=-\infty}^{\infty} F(\omega+n\omega_1) \qquad \ldots. 1.3c$$

where $F(\omega)$ is the Fourier Transform of $f(t)$.

Actually, Linvill gives the relation in terms of the L-transform as:

$$F^*(s) = \frac{1}{T_1}\sum_{n=-\infty}^{\infty} F(s+jn\omega_1) \qquad \ldots. 1.4$$

where $F(s)$ is the Laplace Transform of $f(t)$

and $F^*(s)$ is the Laplace Transform of $f^*(t)$. However, later work by Lago[8] showed that this expression is incomplete and should be modified to read:

$$F^*(s) = \frac{1}{T_1}\sum_{n=-\infty}^{\infty} F(s+jn\omega_1) + f(0^+)/2 \qquad \ldots. 1.5$$

Lago's expression is based on purely physical arguments and is not proven rigorously. However, its validity may be demonstrated by an example.

Consider the input to be a unit step with Laplace Transform 1/s and value at the origin (0^+) of 1. Then equation 1.5 becomes:

$$F^*(s) = \frac{1}{T_1}\sum_{n=-\infty}^{\infty} \frac{1}{s+jn\omega_1} + \frac{1}{2} \qquad \ldots. 1.6$$

The infinite sum in this expression may be written as:

$$\frac{1}{T_1}\sum_{n=-\infty}^{\infty} \frac{1}{s+jn\omega_1} = 2\sum_{n=0}^{\infty} \frac{T_1 s}{(T_1 s)^2+(2n\pi)^2} - \frac{1}{T_1 s} \qquad \ldots. 1.7$$

A similar expression is found in Bromwich's book:[9]

$$\sum_{k=-\infty}^{\infty} \frac{1}{y^2+k^2} = \frac{\pi}{y}\,\frac{\sinh(2\pi y)}{\cosh(2\pi y)-1} \qquad \ldots. 1.8$$

or

$$2\sum_{k=0}^{\infty} \frac{1}{y^2+k^2} = \frac{\pi}{y}\,\frac{\sinh(2\pi y)}{\cosh(2\pi y)-1} + \frac{1}{y^2} \qquad \ldots. 1.9$$

Substituting $y = T_1 s/2\pi$ in 1.4 and simplifying the algebra, expression 1.7 becomes:

$$\frac{1}{T_1}\sum_{n=-\infty}^{\infty}\frac{1}{s+jn\omega_1} = \frac{1}{2}\,\frac{\sinh(T_1 s)}{\cosh(T_1 s)-1} = \frac{1}{2}\coth\left(\frac{T_1 s}{2}\right) \quad \ldots\ldots 1.10$$

and equation 1.6 becomes:

$$F^*(s) = 1/2\,\cosh(T_1 s/2) + 1/2 \quad \ldots\ldots 1.11a$$

$$= 1/2\left[\cosh(T_1 s/2) + 1\right] \quad \ldots\ldots 1.11b$$

$$= e^{T_1 s}/(e^{T_1 s} - 1) \quad \ldots\ldots 1.11c$$

It will be shown later that expression 1.11c is identical to that derived by other methods and is known to be correct. Although this example does not constitute a proof of Lago's equation (1.5) it is more elegant than the example offered in his paper.

The significance of expression 1.3c should be examined. This equation states that the sampling process produces complementary frequencies related in a simple manner to the frequency components of the input signal. If Figure 1.2a represents the frequency spectrum of a hypothetical input to a sampler with sampling period $T_1 = 2\pi/\omega_1$, then the corresponding frequency spectrum of the sampled output is that shown in Figure 1.2b.

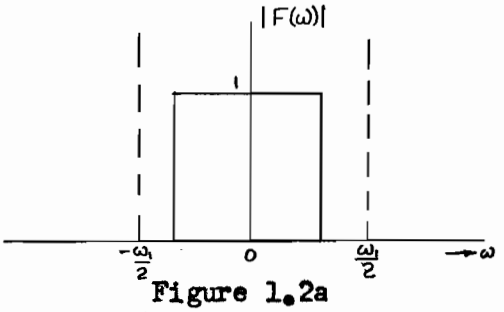

Figure 1.2a

Hypothetical Frequency Spectrum at Sampler Input

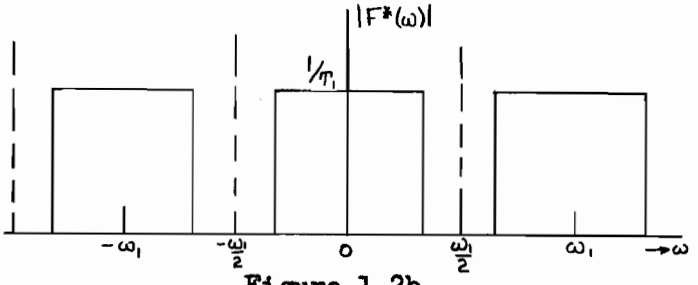

Figure 1.2b

Frequency Spectrum at Sampler Output

Clearly, if the input spectrum contains frequencies higher than $\omega_1/2$, then the complementary spectrum ($n \neq 0$ in equation 1.3) will overlap the primary spectrum ($n = 0$) indicating that the frequencies in the interval

where the overlapping occurs cannot be recovered from the sampled signal. This establishes Shannon's sampling theorem[7]. The input spectrum is assumed to be band-limited to exclude all frequencies higher than half the sampling rate.

1.3 Z-Transform Analysis

The sampling process is represented mathematically by the expression:

$$f^*(t) = f(t) \times \delta_T(t) \qquad \text{.... 1.1}$$

Rather than expand $\delta_T(t)$ in its Fourier series as was done in the frequency-domain analysis, we may write it in terms of its infinite time series:

$$\delta_T(t) = \sum_{n=-\infty}^{\infty} \delta(t - nT) \qquad \text{.... 1.12}$$

where $\delta(t)$ is the unit impulse function and T is the interval between sampling impulses. Furthermore, if $f(t) = 0$ for $t<0$ then equation 1.1 may be rewritten:

$$f^*(t) = f(t) \sum_{n=0}^{\infty} \delta(t - nT) \qquad \text{.... 1.13}$$

Taking the Laplace transform of equation 1.13:

$$F^*(s) = \int_0^{\infty} f(t) \sum_{n=0}^{\infty} \delta(t-nT)\, e^{-sT}\, dt \qquad \text{.... 1.14a}$$

where $F^*(s)$ is the Laplace transform of $f^*(t)$. Assuming absolute convergence of the infinite series, equation 1.14a becomes:

$$F^*(s) = \sum_{n=0}^{\infty} \int_0^{\infty} f(t)\, \delta(t-nT)\, e^{-sT}\, dt \qquad \text{.... 1.14b}$$

$$= \sum_{n=0}^{\infty} f(nT)\, e^{-snT} \qquad \text{.... 1.14c}$$

Substituting $z = e^{sT}$ in the above equation:

$$F(s) = \sum_{n=0}^{\infty} f(nT)\, z^{-n} \qquad \text{.... 1.15}$$

F(z) is called the Z-transform of f(t) but, strictly speaking, it is the Laplace transform of $f^*(t)$ with e^{sT} replaced by z. The foregoing

derivation follows that of Ragazzini and Zadeh[10] who developed the Z-transform in its present form. Equation 1.15 expresses F(z) in an infinite power series in z. It is also possible to determine F(z) in closed form by application of the theory of complex convolution.[11] Jury[12] has done this by taking the complex convolution of F(s), the Laplace transform of f(t) and $(1 - e^{-sT})^{-1}$, the Laplace transform of $\delta_T(t)$. Jury's expression is not reproduced here as equation 1.15 is more amenable to physical interpretation of the sampling process and all necessary results may be derived from it.

The substitution of $e^{sT} = z$ in equation 1.14c to obtain 1.15 is merely a matter of mathematical convenience. The Laplace transform of a sampled function is not analytic in s, but its Z-transform is analytic in z. Conventional techniques may be applied to the analysis of the stability of sampled-data systems by noting that the transformation, $z = e^{sT}$, maps the left half of the s-plane into a unit circle in the z-plane.[12,13]

The applications of the Z-transform are not limited to the analysis of elctric circuits. Just as the Laplace transform may be used to solve linear differential equations, so the Z-transform may be used to solve linear finite difference equations.[14]

The Z-transform of a unit step may be derived as an application of equation 1.15:

$$F(z) = \sum_{n=0}^{\infty} f(nT)\, z^{-n} \qquad \text{.... 1.15}$$

For a unit step, $f(nT) = 1$ for all n, hence

$$F(z) = \sum_{n=0}^{\infty} z^{-n} \qquad \text{.... 1.16a}$$

$$= (1 - z^{-1})^{-1} \qquad \text{.... 1.16b}$$

$$= z/(z-1) \qquad \text{.... 1.16c}$$

With the substitution, $z = e^{sT}$, this expression becomes identical to 1.11c

which confirms the validity of Lago's equation (1.5) for this particular case.

The physical interpretation of equations 1.14c and 1.15, is that they represent a train of impulses starting at t = 0, spaced T seconds apart and with areas equal to the value of the continuous function, f(t), at the sampling instants. In other words, the input signal to the sampler weights the output train of impulses with its value at the sampling instants.

1.4 Z-Transform Algebra

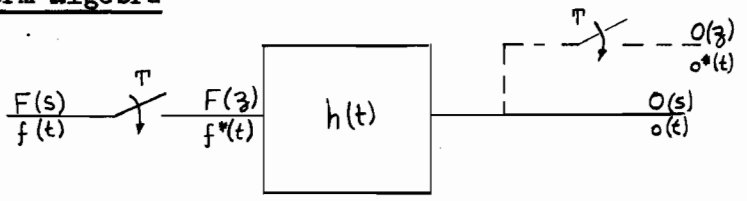

Figure 1.3
A typical linear sampled-data system

In the system shown in Figure 1.3, both the input, f(t), and the output o(t), are sampled in synchronism and h(t) is the impulse response of the system. If the system were continuous, the output would be found by taking the convolution of f(t) with h(t). It will be shown that a similar technique exists for sampled-data systems.

If H(s) is the Laplace transform of h(t), then the output Laplace transform O(s) is:

$$O(s) = F^*(s)\, H(s) \qquad \ldots\ 1.17$$

However, if this output is sampled with a second sampler operating in synchronism with the input sampler, then the output will be O(z), i.e., the Z-transform of o(t). The system impulse response is h(t), therefore at some time mT, the output will be:

$$o(mT) = f(0)h(mT) + f(T)\, h\left[(m-1)T\right] + \ldots + f(mT)\, h(0) \qquad \ldots\ 1.18$$

i.e., the sum of the system responses to that time. This may be written:

$$o(mT) = \sum_{n=0}^{m} f(nT)\, h\left[(m-n)T\right] \qquad \ldots. 1.19$$

Equation 1.19 is called a "convolution summation" and is the sampled-data analog of the convolution integral for a continuous system. The upper summation limit in 1.19 may be extended to infinity because $h\left[(m-n)T\right] = 0$ for $n > m$. As shown:

$$o(mT) = \sum_{n=0}^{\infty} f(nT)\, h\left[(m-n)T\right] \qquad \ldots. 1.20$$

But,

$$O(z) = \sum_{m=0}^{\infty} o(mT)\, z^{-m} \qquad \ldots. 1.21$$

Substituting 1.20 in 1.21 results in:

$$O(z) = \sum_{m=0}^{\infty} \sum_{n=0}^{\infty} f(nT)\, h\left[(m-n)T\right] z^{-m} \qquad \ldots. 1.22a$$

$$= \sum_{n=0}^{\infty} f(nT) \sum_{m=0}^{\infty} h\left[(m-n)T\right] z^{-m} \qquad \ldots. 1.22b$$

$$= \sum_{n=0}^{\infty} f(nT) \sum_{m=0}^{\infty} h\left[(m-n)T\right] z^{-m} \qquad \ldots. 1.22c$$

Where the summation limits have been changed by noting that $h\left[(m-n)T\right] = 0$ for $m<n$. Substituting $k = m-n$ in 1.22c yields:

$$O(z) = \sum_{n=0}^{\infty} f(nT) \sum_{k=0}^{\infty} h(kT)\, z^{-k} z^{-n} \qquad \ldots. 1.23a$$

$$= \sum_{n=0}^{\infty} f(nT)\, z^{-n} \sum_{k=0}^{\infty} h(kT)\, z^{-k} \qquad \ldots. 1.23b$$

$$= F(z)\, H(z) \qquad \ldots. 1.23c$$

Thus, the Z-transform of the output of a linear sampled-data system with the configuration of Figure 1.3 is the product of the Z-transform of the input signal with the Z-transform of the system impulse response. The algebra for other system configurations has been well developed and may be found in numerous sources.[4,10,13,14]

The sampled output, $o^*(t)$, may be determined by expanding $O(z)$ in inverse powers of z and examining the coefficients of the various terms which give the value of $o(t)$ at the sampling instants. Alternatively, $o^*(t)$ may be obtained in closed form by taking the inverse Z-transform.[12,13]

The theory which has been developed thus far will yield the value of the output at the sampling instants, but will not indicate how the system behaves between samples. In some cases, this may be all that is necessary to determine the stability of a sampled-data control system or to aid in the synthesis of such a system. However, in the problem with which this research is concerned, this property of the Z-transform seriously limits its usefulness.

1.5 The Modified Z-Transform

To obtain the response of a sampled-data system between sampling instants, an extension of the Z-transform, called the modified Z-transform, has been developed.[15,16,17] This transform is evaluated by considering the effect of introducing a fictitious time delay ΔT ($\Delta<1$) in a linear sampled-data system.

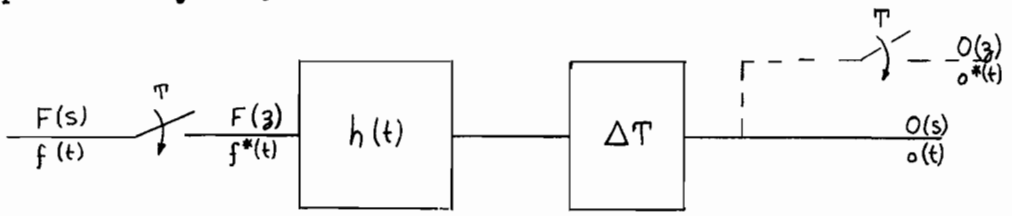

Figure 1.4

Sampled-Data System with Fictitious Time Delay ΔT

The manner of introducing the fictitious delay is shown in Figure 1.4, and the effect ot this delay on the system output is illustrated in Figure 1.5.

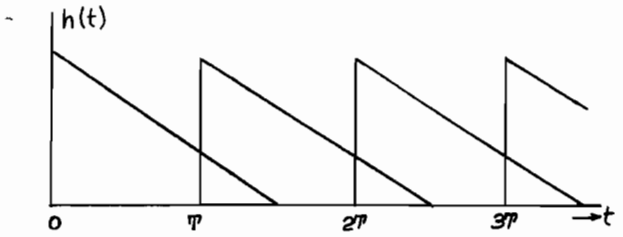

Figure 1.5a

Hypothetical System Response with no Delay

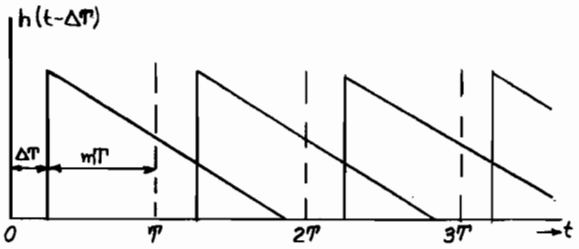

Figure 1.5b

Effect of a Delay ΔT on the System Response of Figure 1.5a

Figure 1.5 shows that the sampled output, O(z), of the circuit in Figure 1.4 will give the value of the undelayed output at $(n - \Delta)T$ when the sample is taken at nT. If we define $m = 1-\Delta$ $(m<1)$, then the output at the sampling instants of the system with the fictitious delay will be the value of the undelayed output at $(n - 1)T + mT$, and thus:

$$o(nT) = f(0)\, h\left[(n + m - 1)T\right] + \ldots + f\left[(n - 1)T\right] h(mT) \qquad \ldots. 1.24$$

or, $$o(nT) = \sum_{k=0}^{n-1} f(kT)\, h\left[(n + m - k - 1)T\right] \qquad \ldots. 1.25$$

Now, $h\left[(n + m - k - 1)T\right] = 0$ for $k > n - 1$, so the upper summation limit may be extended to infinity. Doing this, and substituting the resulting expression in 1.21:

$$O(z) = \sum_{n=0}^{\infty} \sum_{k=0}^{\infty} f(kT)\, h\left[(n + m - k - 1)T\right] z^{-n} \qquad \ldots. 1.26$$

Substituting $p = n - k - 1$, and noting that $h\left[(p + m)T\right] = 0$ for $p<0$, results in the expression:

$$O(z) = \sum_{k=0}^{\infty} f(kT) \sum_{p=0}^{\infty} h\left[(p + m)T\right] z^{-p} z^{-k} z^{-1} \qquad \ldots. 1.27a$$

$$= \sum_{k=0}^{\infty} f(kT)\, z^{-k}\, z^{-1} \sum_{p=0}^{\infty} h\left[(p + m)T\right] z^{-p} \qquad \ldots. 1.27b$$

$$= F(z)\, H(z,m) \qquad \ldots. 1.27c$$

where $$H(z,m) = z^{-1} \sum_{n=0}^{\infty} h\left[(n + m)T\right] z^{-n} \qquad \ldots. 1.28$$

Cheng[14] defines H(z,m) as $H(z,m) = \sum_{n=0}^{\infty} h(nT + mT)\, z^{-n}$ and calculations using this expression agree with those to be found in Lago's paper,[18] but the definition of equation 1.28 will be used as it is the one generally found in the literature on this subject.

As neither the fictitious delay nor the second sampler is actually present in a practical sampled-data system, it is conventional to use the notation

$$O(z,m) = F(z)\, H(z,m) \qquad \ldots. 1.29$$

where O(z,m) is the modified Z-transform of the output and H(z,m) is the modified Z-transform of the system transfer function. The algebra for

other system configurations may be found in numerous sources.[13,17]

The complete system response may be found by taking the inverse transform of O(z,m) and allowing m to vary between 0 and 1. The time domain response is obtained by substituting t = (n-1+m)T in the inverse transform.

From an examination of equation 1.28, it is seen that:

$$\lim_{m\to 0} z\,H(z,m) = H(z)$$

Thus, multiplying O(z,m) by z and allowing $m\to 0$, we obtain the upper value of the system response at the sampling instants, i.e, the value at $0^+, T^+, 2T^+ \ldots$ If we allow $m\to 1$ in the expression for O(z,m), we obtain the value of the output at $0^-, T^-, 2T^-, \ldots$. If the system has a continuous impulse response, the following relation exists:

$$\lim_{m\to 0} z\,H(z,m) = \lim_{m\to 1} H(z,m)$$

now

$$\lim_{m\to 1} H(z,m) = \lim_{m\to 0} z\,H(z,m) - h(0)$$

Therefore, the system can only have a continuous impulse response if $\lim_{t\to 0} h(t) = 0$. By the initial value theorem for Laplace Transforms this is equivalent to the relation:

$$\lim_{s\to\infty} s\,H(s) = 0 \qquad \ldots. 1.30$$

If H(s) can be expressed as the ratio of two polynomials in s, then the polynomial in the denominator must be of a degree at least two greater than the degree of the polynomial in the numerator, to satisfy equation 1.30.

The modified Z-transform may also be used to express certain infinite series in closed form.[17] This is done by noting that:

$$o(t) = L^{-1}(F^*(s)\,H(s))$$

where L^{-1} denotes the inverse Laplace transform. Evaluating o(t) by taking the inverse Laplace transform will result in an expression in infinite series form. o(t) may also be evaluated by taking the inverse transform of

$O(z,m)$ and putting $t = (n - 1 + m)T$. This will yield an expression for $o(t)$ in closed form. The two forms of $o(t)$ must be identical as they describe the same system and the modified Z-transform is just a special case of the Laplace transform.

1.6 The P-Transform

The methods of the Z-transform and the modified Z-transform are applicable to the analysis of sampled-data systems where the sampling impulses have zero width. Results obtained by the use of these methods are exact only if the sampler transforms the finite amplitude of the input signal to true impulses of equivalent area, which is physically impossible. An analysis of the effect of the finite width of the sampling pulses has been made by Farmanfarma[19,20,21] and has resulted in the definition of the P-Transform.

The P-Transform of a continuous signal, $f(T)$, which is sampled by pulses of width h, is defined as the Laplace transform of the product of $f(t)$ and the train of sampling pulses, each of unit height, width h, and occuring periodically every T seconds. The P-Transform is obtained by taking the complex convolution of $F(s)$, which is the Laplace transform of $f(t)$, with $(1 - e^{-hs})\, s^{-1}(1 - e^{-sT})^{-1}$, the Laplace transform of the pulse train. Tables of P-transforms will be found in Farmanfarma's paper[19] and Jury's book.[13]

An analysis has also been made by the author similar to that for the derivation of the Z-transform in infinite series form. However, as the resulting expression involves both integration and summation, it offers no advantage in the physical interpretation of the sampling process over Farmanfarma's expression.

For the open-loop system already discussed in some detail, the modified Z-transform of the output is

$$O(z,m) = F(z)\, H(z,m) \qquad \ldots\ldots 1.29$$

The time domain response is then obtained by taking the inverse transform of $O(z,m)$. When the finite pulse width is taken into consideration, the corresponding expression becomes:

$$O(s) = F_p(s)\, H(s) \qquad \ldots\ldots 1.31$$

where $F_p(s)$ is the P-transform of the input, $f(t)$. The time domain response may be found in closed form by taking the inverse P-transform of $O(s)$.

The greatest inaccuracies in using the Z-transform when the sampling pulses have a finite width occur when the system has a discontinuous impulse response, i.e. equation 1.30 is not satisfied. Under these conditions, the Z-transform predicts a finite discontinuity at the sampling instants, while the P-transform predicts a continuous output with a finite discontinuity in its first derivative at the beginning and end of each sampling pulse. Large errors will be incurred in predicting any system response with the Z-transform if the sampling pulse width is comparable to the system time constant.

The frequency domain analysis of a signal sampled by a pulse of finite width may be accomplished by a method similar to that used for the case of ideal impulses.

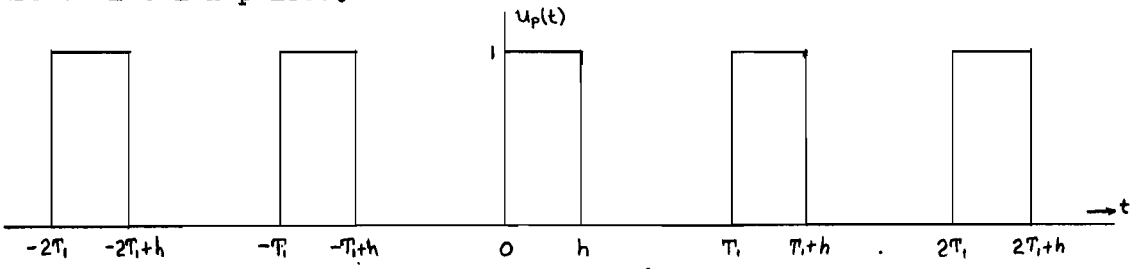

Figure 1.6

The Sampling-Pulse Train

If Figure 1.6 respresents the train of sampling pulses, its finite Fourier transform is:

$$U_p(\omega) = \frac{1}{T_1}\int_0^h e^{-jn\omega_1 t}\,dt \qquad \text{.... 1.32a}$$

$$= \left(1 - e^{-jn\omega_1 h}\right)/jn\omega_1 T_1 \qquad \text{.... 1.32b}$$

where $\omega_1 = 2\pi/T_1$. The sampling pulse function, $u_p(t)$, may now be expanded in a complex Fourier series.

$$u_p(t) = \sum_{n=-\infty}^{\infty} U_p(\omega_1)\, e^{jn\omega_1 t} \qquad \text{.... 1.33a}$$

$$= \frac{1}{2\pi j}\sum_{n=-\infty}^{\infty}{}' \frac{1 - e^{-jn\omega_1 h}}{n}\cdot e^{jn\omega_1 t} + \frac{h\omega_1}{2\pi} \qquad \text{.... 1.33b}$$

where $\sum'$ means that the term n = 0 is excluded from the summation. The Fourier transform of the sampled output, $F_p^*(\omega)$, may now be evaluated using the method of section 1.2

$$F_p^*(\omega) = \frac{1}{2\pi j}\sum_{n=-\infty}^{\infty}{}' \int_{-\infty}^{\infty} \frac{f(t)\,(1 - e^{-jn\omega_1 h})}{n}\cdot e^{jn\omega_1 t} e^{-j\omega t}\,dt + F(\omega)\frac{h\omega_1}{2\pi} \qquad \text{.... 1.34a}$$

Substituting k = -n:

$$F_p^*(\omega) = \frac{1}{2\pi j}\sum_{k=-\infty}^{\infty}{}' \frac{(1 - e^{jk\omega_1 h})}{-k}\int_{-\infty}^{\infty} f(t)\, e^{-j(\omega + k\omega_1)t}\,dt + F(\omega)\frac{h\omega_1}{2\pi} \qquad \text{.... 1.34b}$$

$$= \frac{-1}{2\pi j}\sum_{n=-\infty}^{\infty}{}' F(\omega + n\omega_1)\,\frac{1 - e^{jn\omega_1 h}}{n} + F(\omega)\,\frac{h\omega_1}{2\pi} \qquad \text{.... 1.34c}$$

where $F(\omega)$ is the Fourier transform of $f(t)$ and $\omega_1 = 2\pi/T_1$.

The foregoing analysis is quite different from that of Farmanfarma who obtains the result

$$F_p^*(s) = \frac{-1}{2\pi j}\sum_{k=-\infty}^{\infty}{}' F(s + jk\omega_1)\,\frac{1 - e^{jk\omega_1 h}}{k} + F(s)\,\frac{h\omega_1}{2\pi} \qquad \text{.... 1.35}$$

where $F(s)$ is the Laplace transform of $f(t)$ and $F_p^*(s)$ is the Laplace transform of the sampled output.

Expressions 1.34c and 1.35 may be reduced to their corresponding

forms for the case of zero pulse width by letting the amplitude of the sampling pulses equal $1/h$ instead of unity and then letting $h \to 0$. It is also noted that in the limit as $h \to T$, the equations become

$$\lim_{h \to T} F_p^*(\omega) = F(\omega)$$

$$\lim_{h \to T} F_p^*(s) = F(s)$$

as would be expected.

The physical significance of equation 1.34c is illustrated for the case $h/T = 0.25$ in Figures 1.7a and 1.7b, which show the power spectrum of a hypothetical signal before and after sampling. It is seen that a given complementary frequency is attenuated by the factor $h(\sin x)/x$ over its corresponding value in Figure 1.2b, where $x = n\pi h/T$ and n is the order of the complementary component. Shannon's sampling theorem still applies.

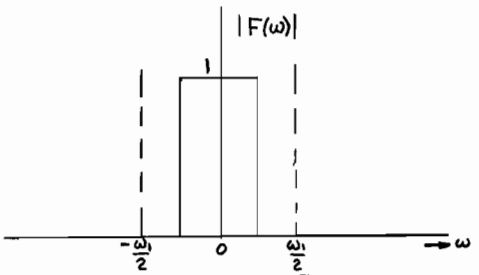

Figure 1.7a

Hypothetical frequency spectrum at sampler input.

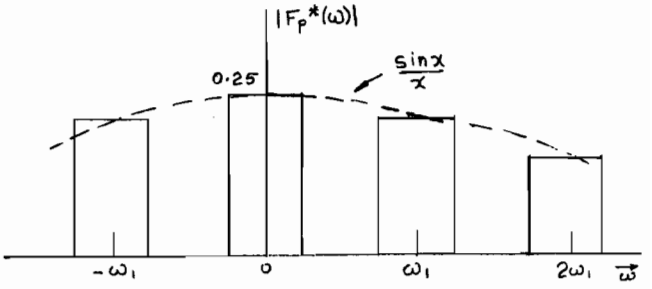

Figure 1.7b

Frequency spectrum after sampling by a finite-width pulse.

1.7 Sampled-Data Filters

In addition to the work already discussed relating to sampled-data control systems, much interest has been shown recently in sampled-data filters. These may be of many configurations and one type is the n + m port network with n inputs where sampled-data signals are applied and m outputs which supply continuous signals related by weighting functions, W_{ij}, to the n inputs. If the general nature of the input signal is

known, and the desired nature of the output signal is specified, then the weighting functions may be determined according to some criterion such as optimization in the Wiener sense.[22,23]

Another type of filter which seems to have many applications is the N-path filter described by Franks and Sandberg.[24] For the particular case where the inputs are pulse modulated, this may be considered a sampled-data filter. An application of sampled-data filtering to self-optimizing systems has also been reported.[25]

1.8 Scope and Purpose of the Research Undertaken

Many theoretical investigations have been made in the analysis and synthesis of sampled-data control systems and sampled-data filters. However, with a few notable exceptions,[25] the reporting of experimental verification and complementing of these results have not kept pace with theoretical developments, although such studies are probably being conducted in areas not generally discussed in available literature.

One reason for this situation could be the lack of suitable university laboratory simulation facilities, which are available to the individual research worker. Simple sampled-data control systems may be studied by means of an analog computer and a motor-driven rotary switch, but this arrangement sets an upper limit to the sampling rate which may be used, and does not permit the investigation of sampled-data filters requiring a memory to store values of past samples. It is true that some authors[26,27] have described laboratory models for studying sampled-data systems, but their methods have limited flexibility.

The purpose of this research is two-fold: the analytical and experimental investigation of certain aspects of a type of sample-data

filter.

Analytical studies have resulted in some alternate derivations of theorems in sampled-data theory already discussed in this chapter. A general expression for the transfer function of the class of filters called finite-memory hold-circuits has also been established. This will be considered in the next chapter.

The experimental investigations have dealt with methods of simulating these sampled-data filters and at the same time considered the requirements which must be satisfied by the components of a sampled-data simulation scheme. The actual building of these filters will be left for a future investigation as this phase of the research is concerned only with the feasibility of certain simulation techniques and indicates which components will require more development before an operational filter is built.

CHAPTER II

RESTORATION OF SAMPLED-DATA SIGNALS

2.1 Low-Pass Filtering

In most sampled-data systems, the input is pulsed, while the plant has been designed to respond to a continuous input. Although "plant" is a term generally reserved for control systems, it may also be interpreted in this context as the read-out devices in a telemetering system. Therefore, before the sampled input is applied to the plant, it must be demodulated or restored to a continuous signal which should be a facsimile of the original signal. Although Ragazzini and Zadeh[10] observe that the digital signal may somtimes be applied directly to the plant, they nevertheless recommend that a restoring circuit be placed between the plant and the sampled input. Thus the study of sampled-data restoration circuits is an important field for investigation.

An examination of Figure 1.2 and associated equation 1.3c immediately suggests one method of accomplishing the necessary restoration. If an ideal low-pass filter could be built with zero attenuation over the range $|\omega|<\omega_1/2$ and infinite attenuation for $|\omega|>\omega_1/2$, then this filter would remove all complementary frequency components from the sampled-signal spectrum, leaving only the primary components which are those of the original signal. Such an ideal filter can only be approximated, of course, and much has been written on the design of such filters. Once such a filter has been designed and its transfer function evaluated, its performance in a given system may be predicted by using the Z-transform or P-transform analysis. It should be noted that such a filter must have a continuous impulse response as defined by equation 1.30 for a smooth output.

One drawback of these filters is the inevitable phase-shift introduced in the output signal. In time-shared communication links and certain telemetering systems such a phase-shift is not important, but in control systems, this phase-shift may lead to instability. For this reason, these filters are seldom used as restoration elements in sampled-data control systems. Nevertheless, devices which are used do have low-pass filtering characteristics.

2.2 The Zero Order Hold Circuit

Ragazzini and Zadeh[10] suggest the use of a hold circuit to restore the digital signal to an analog form. The function of a hold circuit is to reconstruct approximately the original time function from the impulse train generated by the sampler. The simplest hold circuit is the zero order hold, sometimes called a clamp circuit or boxcar generator. The operation of this circuit is shown in Figure 2.1.

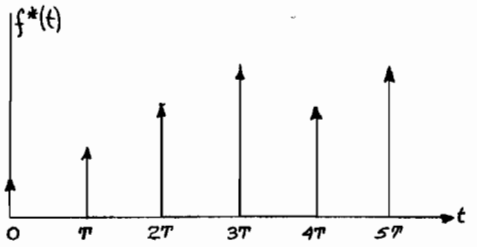

Figure 2.1a

Hypothetical Sampler Output

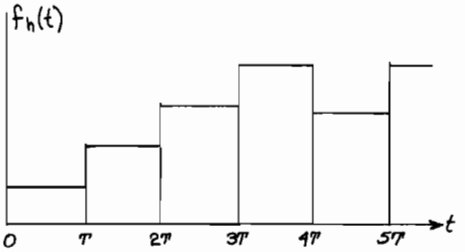

Figure 2.1b

Ideal Hold Output

The zero order hold maintains its output constant at the value of the last sample until a new sample is received, whereupon the output changes discontinuously to the new sample value. If the continuous input function, f(t), is expanded in a Taylor's series about the point nT, the resulting expression is:

$$f(t) = f(nT) + f'(nT)\,(t-nT) + \frac{f''(nT)}{2!}\,(t-nT)^2 + \ldots \qquad \ldots. \; 2.1$$

where the primes indicate the derivatives of f(t) at $t_n = nT$. The zero order

hold approximates f(t) by the first term in this expansion:

$$f_h(t) = f(nT) \ , \quad nT \leq t < (n+1)T \qquad \ldots. \ 2.2$$

where $f_h(t)$ is the hold circuit output. The transfer function of such a hold circuit is:[10]

$$G_0(s) = (1 - e^{-sT})/s \qquad \ldots. \ 2.3$$

and

$$\left|G_0(j\omega)\right| = \frac{2}{\omega}\left|\sin\frac{\omega T}{2}\right| \qquad \ldots. \ 2.4$$

where T is the sampling period. Relation 2.4 is plotted in Figure 2.2 which shows that this circuit has low-pass filtering characteristics.

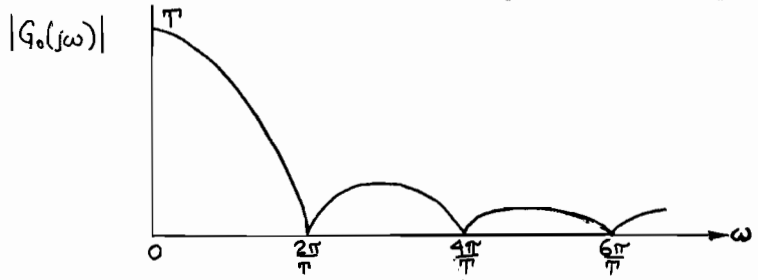

Figure 2.2

Frequency Response of the Zero-Order Hold

Restoration of sampled-data by hold circuits is essentially a digital operation, requiring a memory to store the values of past samples which are required to generate the continuous output. The zero-order hold may be considered as a member of a class of sampled-data filters embracing all hold circuits.

It is seen that the transfer function for the zero-order hold (equation 2.3) does not satisfy the requirements for a continuous impulse response (equation 1.30) and hence its output will have finite discontinuities at the sampling instant as shown in Figure 2.1.

2.3 Analysis of Systems with Hold Circuits

Figure 2.3 shows a typical sampled-data system employing a zero-order hold as a restoring element.

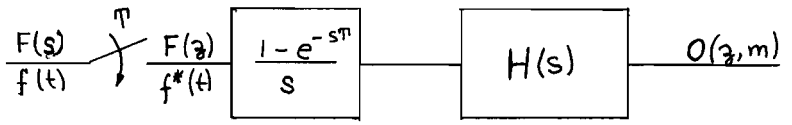

Figure 2.3

Typical Sampled-Data System Employing a Zero-Order Hold

From equation 1.27c, the output of this system is:

$$O(z,m) = F(z)\, T(z,m) \qquad \text{.... 2.5}$$

where T(z,m) is the modified Z-transform of

$$T(s) = (1 - e^{-sT})\, H(s)/s \qquad \text{.... 2.6}$$

Consider transfer functions of the form

$$G_1(s) = G(s)\, e^{-ksT} \qquad \text{.... 2.7}$$

where k is an integer. This is the same as a circuit with a transfer function G(s) followed by an element introducing a delay of kT seconds. From equation 1.28, the modified Z-transform of equation 2.7 is:

$$G_1(z,m) = z^{-1} \sum_{n=0}^{\infty}{}' g_1\left[(n+m)T\right] z^{-n} \qquad \text{.... 2.8}$$

Now, $g_1(t) = g(t - kT)$ for $t \geqslant kT$

$= 0$ for $t < kT$

Therefore, $G_1(z,m) = z^{-1} \sum_{n=0}^{\infty}{}' g\left[(n+m-k)T\right] z^{-n}$ 2.9

Substituting $j = n - k$, this becomes

$$G_1(z,m) = z^{-1} \sum_{j=-k}^{\infty}{}' g\left[(j+m)T\right] z^{-j} z^{-k} \qquad \text{.... 2.10a}$$

$$= z^{-1} z^{-k} \sum_{j=0}^{\infty}{}' g\left[(j+m)T\right] z^{-j} \qquad \text{.... 2.10b}$$

where the lower summation limit has been changed because

$$g(j+m) = 0 \quad \text{for } j+m < 0$$

$$\lim_{m \to 1} g(m-1) = g(0^-) = 0 \text{ by definition.}$$

Hence, $$G_1(z,m) = z^{-k}\, G(z,m) \qquad \text{.... 2.11}$$

and, $$T(z,m) = (1 - z^{-1})\, Z_m\left[H(s)/s\right] \qquad \text{.... 2.12}$$

where $Z_m\left[H(s)/s\right]$ is the modified Z-transform of $H(s)/s$. Equation 2.5 may now

be rewritten:

$$O(z,m) = (z - 1)/z\ F(z)\ Z_m\left[H(s)/s\right] \qquad \text{.... 2.13}$$

The use of a zero-order hold results in very little additional complication of the basic equations describing the sampled-data behaviour of a plant with transfer function H(s). Furthermore, the system in Figure 2.3 will have a continuous impulse response if $\lim_{S\to\infty} H(s) = 0$. If the hold circuit only responds to the value at the start of a finite-width sampling pulse, which may be considered the ideal behaviour, the Z-transform analysis of equation 2.13 is still valid even though the sampling pulses have a finite width.

2.4 First Order Hold Circuits

Although most papers on sampled-data systems consider only the zero-order hold as a sampled-data restoration element, its principle may be extended to circuits which approximate the continuous function by a polynomial in t whose coefficients are determined by the sample values. For example, a first order hold would yield an output with the form:

$$f_h(t) = f(nT) + \frac{(t - nT)}{T}\left\{f(nT) - f\left[(n-1)T\right]\right\} \qquad \text{.... 2.14}$$

for $nT \leqslant t < (n+1)T$.

Such a hold circuit is described by Jury[13] and its operation is shown in Figure 2.4. Its transfer function is:

$$G_1(s) = (1 - e^{-sT})^2\left[1/s + 1/(Ts^2)\right] \qquad \text{.... 2.15}$$

When a first order hold circuit is used in the system in Figure 2.3 instead of a zero-order hold, the coresponding equation describing the operation of the system is:

$$O(z,m) = \left[\frac{z-1}{z}\right]^2 F(s)\left\{Z_m\left[H(s)/s\right] + \frac{1}{T}\,Z_m\left[H(s)/s^2\right]\right\} \qquad \text{.... 2.16}$$

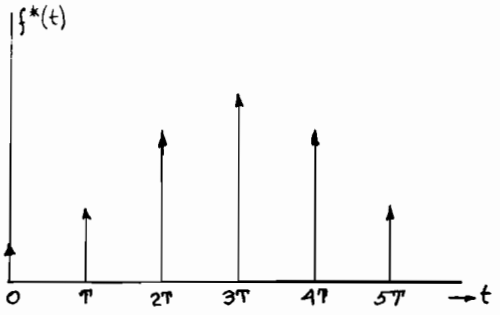

Figure 2.4a

Hypothetical Sampler Output

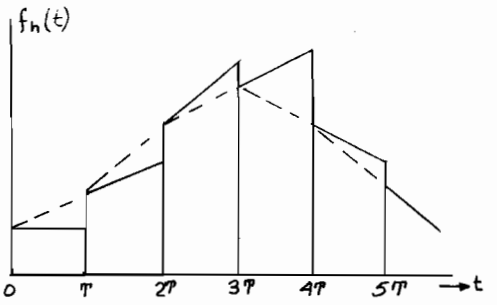

Figure 2.4b

First-Order Hold Output

The general expression for the output of a hold circuit may now be given:

$$f(nT + t) = a_0 + a_1 t + a_2 t^2 + \ldots + a_n t^n + \ldots \quad ..2.17$$

for $0 \leq t < T$. The a_i are parameters determined by past samples and are constant in any sampling interval.

2.5 Generalized Hold Circuits

The physical operation of a generalized hold circuit may be visualized by considering it to be a predicting circuit which fits a polynomial of finite degree to past sample values and then extrapolates this function over a sampling interval. The hold circuit output consists only of the extrapolated portion of the function and the degree of the coresponding polynomial is governed by the number of past samples which subsequently determine the a_i parameters in equation 2.17.

A hold circuit will be defined to be of order p if the polynomial in equation 2.17 is of degree p. This definition agrees with that for the zero and first-order hold circuits already discussed. To generate such a polynomial, the hold circuit must contain a memory capable of storing p + 1 sample values and be able to perform mathematical operations with these quantities to generate the required polynomial. We are at liberty to define another parameter relating to hold circuits: this is its rank, a term which has not been previously reported in the literature. If the output of a hold

circuit is a polynomial of degree p, but the coefficient a_p is calculated from p + q + 1 sample values, then the hold circuit is said to have rank q. This quantity is the number of excess sample values over the minimum, p + 1, required by the degree of the polynomial approximation. Conventional hold circuits have a rank of zero. The notation for a generalized hold circuit will be (p,q) where p is its order and q is its rank.

The physical meaning of the terms, "order" and "rank", may be illustrated with the aid of Figures 2.5a and 2.5b. The former shows a first-order, zero-rank filter output for an arbitrary set of samples; the latter illustrates a first-order, first-rank output for the same set of samples.

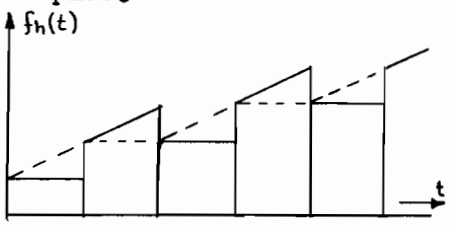

Figure 2.5a

Hypothetical (1,0) hold output

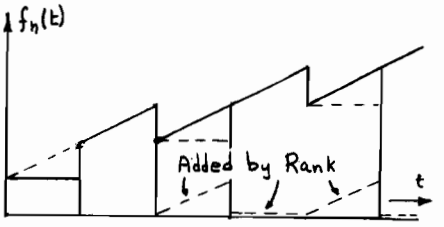

Figure 2.5b

Corresponding (1,1) hold output

In both cases, the filter output consists of ramps with abrupt discontinuities at the sampling instants. In Figure 2.5a, the slope of the ramp is determined by two samples, while in the other figure, this quantity is determined by three samples.

The generation of a polynomial for the restoration of sampled-data is not a new concept, having already been described by Porter and Stoneman.[28] In their method, a polynomial of the r^{th} degree is generated by cascading r integrators whose initial conditions or displacements are adjusted at each sampling instant in accordance with some predetermined scheme. Their method requires only one memory unit which stores the algebraic sum of past samples, the output of this unit being multiplied by appropriate scaling factors before

being applied to the integrators. The stability of their system was later investigated by Lawden.[29]

The approach to the design of hold circuits which has been used in this research is quite different from that of Porter and Stoneman. The generalized (p,q) hold circuit is considered to have a memory capable of storing p + q + 1 sample values so that values of the individual samples and not just their sum may be utilized by the computing section of the device. The hold circuit is considered to be a sampled-data filter and a general expression for the transfer function of a hold circuit of arbitrary order and rank is evaluated. This may be considered to be the transfer function of the filter to a sampled-input and is of such a form that a system containing these hold circuits may be readily analysed by the Z-transform.

The use of a large but finite memory in the filter greatly increases its flexibility because polynomials of a given maximum order may be generated according to a variety of criteria. The filter may be interconnected in such a way as to generate a polynomial to fit a given input with the same accuracy as a Porter-Stoneman system.

Finally, electronic analog computing elements are used exclusively in the construction of the finite-memory hold circuits. Most of Porter and Stoneman's work was done with mechanical differential analysers although they reported a two integrator model which used an electronic integrator and a Velodyne integrator. All-electronic circuitry such as used here, provides a more flexible simulation scheme.

2.6 Analysis of Generalized Hold Circuits

The analysis of the generalized hold circuit can most easily be

accomplished by the use of the calculus of finite differences. We shall therefore define the necessary operators which will be needed.

Generally, $\Delta f(nT)$ is the notation for the first descending difference[30] of $f(nT)$, and $\nabla f(nT)$ is the notation for the first ascending difference.[30] However, as the first quantity is not used in the problem at hand, the following notation will be adopted:

$$\Delta f(nT) = f(nT) - f\left[(n-1)T\right] \quad \ldots\ldots 2.18a$$

$$\Delta^2 f(nT) = \Delta f(nT) - \Delta f\left[(n-1)T\right] \quad \ldots\ldots 2.18b$$

$$\Delta^k f(nT) = \Delta^{k-1} f(nT) - \Delta^{k-1}\left[(n-1)T\right] \quad \ldots\ldots 2.18c$$

The symbolic operator E^r, when applied to $f(nT)$, increases its argument by rT:

$$E^r f(nT) = f\left[(n+r)T\right] \quad \ldots\ldots 2.19a$$

$$E^{-r} f(nT) = f\left[(n-r)T\right] \quad \ldots\ldots 2.19b$$

With this notation, equation 2.18a becomes:

$$\Delta f(nT) = f(nT) - E^{-1} f(nT) \quad \ldots\ldots 2.20a$$

$$= (1 - E^{-1}) f(nT) \quad \ldots\ldots 2.20b$$

It is convenient to abbreviate the above by writing:

$$\Delta = 1 - E^{-1} \quad \ldots\ldots 2.21$$

the operand, $f(nT)$, on each side being understood.

We may generalize equation 2.21 by writing

$$\Delta^p = (1 - E^{-1})^p \quad \ldots\ldots 2.22a$$

By the binomial theorem, this becomes

$$\Delta^p = \sum_{r=0}^{p} (-1)^r \binom{p}{r} E^{-r} \quad \ldots\ldots 2.22b$$

where $\binom{p}{r} = \dfrac{p!}{(p-r)!\ r!}$

or alternatively, $$\Delta^p f(nT) = \sum_{r=0}^{p} (-1)^r \binom{p}{r} f\left[(n-r)T\right] \quad \ldots\ldots 2.23$$

Introducing the symbols:

$$\delta_n^p = \Delta^p f(nT)$$

$$f(n_rT) = f\left[(n - r)T\right]$$

equation 2.23 may be re-written:

$$\delta_n^p = \sum_{r=0}^{p}(-1)^r\binom{p}{r}f(n_rT) \qquad \text{.... 2.24}$$

The particular form of (p,q) hold circuit considered here is that whose output is described by equation 2.25:

$$f_h(t) = f(nT) + \frac{\delta_n^1}{T}(t - nT) + \ldots + \frac{\delta_n^p\,(t - nT)^p}{T^p} + \frac{(t - nT)^p}{T^p}\sum_{r=1}^{q} R_r\,\delta_n^{p+r} \qquad \text{.. 2.25}$$

for $nT \le t < (n+1)T$

where the R_r are predetermined constants called the rank coefficients.

The total output is the sum of terms of this type over all values of n from 0 to ∞. The Laplace transform of this output, divided by the Laplace transform of the input, will given the transfer function of the sampled-data filter. If $F_h(s)$ is the Laplace transform of the hold circuit output, $\sum_n f_h(t)$, then we have the relation:

$$F_h(s) = \sum_{n=0}^{\infty}\int_{nT}^{(n+1)T}\left\{\sum_{r=0}^{p}\delta_n^r\frac{(t - nT)^r}{T^r} + \frac{(t - nT)^p}{T^p}\sum_{r=1}^{q}R_r\,\delta_n^{p+r}\right\}e^{-st}dt \qquad \text{.... 2.26a}$$

The summation and integral signs may be interchanged, and $x = t - nT$ substituted in the integrals, with the result:

$$F_h(s) = \sum_{n=0}^{\infty}\left\{\sum_{r=0}^{p}\frac{\delta_n^r}{T^r}\int_0^T x^r\,e^{-sx}e^{-snT}dx + \int_0^T x^p e^{-sx}e^{-snT}\,dx\sum_{r=1}^{q}\frac{R_r\delta_n^{p+r}}{T^p}\right\} \qquad \text{.... 2.26b}$$

Formula 567.9 in Dwight's "Table of Integrals"[31] may be applied to evaluate the integral in equation 2.26b, with the result:

$$\int_0^T x^r\,e^{-sx}dx = e^{-sx}\sum_{j=0}^{r}\frac{r!\,x^{r-j}}{(r-j)!\,s^{j+1}}\Bigg|_0^T \qquad \text{.... 2.27}$$

$$= \frac{r!}{s^{r+1}} - e^{-sT}\sum_{j=0}^{r}\frac{r!\,T^{r-j}}{(r-j)!\,s^{j+1}} \qquad \text{.... 2.28}$$

Substituting equation 2.28 in expression 2.26b, we get the relation:

$$F_h(s) = \sum_{n=0}^{\infty}\left\{\sum_{r=0}^{p}\frac{\delta_n^r}{T^r}e^{-snT}\left[\frac{r!}{s^{r+1}} - e^{-sT}\sum_{j=0}^{r}\frac{r!\,T^{r-j}}{(r-j)!\,s^{j+1}}\right]\right.$$

$$\left. + e^{-snT}\left[\frac{p!}{s^{p+1}} - e^{-sT}\sum_{j=0}^{p}\frac{p!\,T^{p-j}}{(p-j)!\,s^{j+1}}\right]\sum_{r=1}^{q}R_r\,\frac{\delta_n^{p+r}}{T^p}\right\} \qquad \text{.... 2.29}$$

Consider the evaluation of the sum $\sum_{n=0}^{\infty} \delta_n^r e^{-snT}$, subject to the condition $f(n_rT) = 0$ for $n<r$. Substituting equation 2.24 for δ_n^r we get:

$$\sum_{n=0}^{\infty} \delta_n^r e^{-snT} = \sum_{n=0}^{\infty} e^{-snT} \sum_{j=0}^{r} (-1)^j \binom{r}{j} f(n_jT) \quad \text{.... 2.30a}$$

Interchange summation signs and substitute $m = n - j$:

$$\sum_{n=0}^{\infty} \delta_n^r e^{-snT} = \sum_{j=0}^{r} (-1)^j \binom{r}{j} \sum_{m=-j}^{\infty} f(mT)\, e^{-sjT}\, e^{-smT} \quad \text{.... 2.30b}$$

But, $f(mT) = 0$ for $m<0$, so the sum becomes:

$$\sum_{n=0}^{\infty} \delta_n^r e^{-snT} = \sum_{j=0}^{r} (-1)^j \binom{r}{j} \sum_{m=0}^{\infty} f(mT)\, e^{-sjT}\, e^{-smT} \quad \text{.... 2.30c}$$

$$= \sum_{m=0}^{\infty} f(mT)\, e^{-smT} \sum_{j=0}^{r} (-1)^j \binom{r}{j} e^{-sjT} \quad \text{.... 2.30d}$$

By the binomial theorem, the second sum becomes:

$$\sum_{j=0}^{r} (-1)^j \binom{r}{j} e^{-sjT} = (1 - e^{-sT})^r \quad \text{.... 2.31}$$

The Laplace transform of the hold circuit may now be simplified:

$$F_h(s) = \sum_{m=0}^{\infty} f(mT)\, e^{-smT} \left\{ \sum_{r=0}^{p} \frac{(1 - e^{-sT})^r}{T^r} \left[\frac{r!}{s^{r+1}} - e^{-sT} \sum_{j=0}^{r} \frac{r!\, T^{r-j}}{(r-j)!\, s^{j+1}} \right] \right.$$

$$\left. + \frac{1}{T^p} \left[\frac{p!}{s^{p+1}} - e^{-sT} \sum_{j=0}^{p} \frac{p!\, T^{p-j}}{(p-j)!\, s^{j+1}} \right] \sum_{r=1}^{q} R_r (1-e^{-sT})^{p+r} \right\} \quad \text{.... 2.32}$$

The transfer function of the filter may now be found by dividing equation 2.32 by the Laplace transform of the input. From equation 1.14c, the Laplace transform of the input is $F^*(s) = \sum_{m=0}^{\infty} f(mT)\, e^{-smT}$. Therefore, the transfer function of a (p,q) hold circuit, denoted by $G_{p,q}(s)$ is:

$$G_{p,q}(s) = \sum_{r=0}^{p} \frac{(1 - e^{-sT})^r}{T^r} \left[\frac{r!}{s^{r+1}} - e^{-sT} \sum_{j=0}^{r} \frac{r!\, T^{r-j}}{(r-j)!\, s^{j+1}} \right]$$

$$+ \frac{1}{T^p} \left[\frac{p!}{s^{p+1}} - e^{-sT} \sum_{j=0}^{p} \frac{p!\, T^{p-j}}{(p-j)!\, s^{j+1}} \right] \sum_{r=1}^{q} R_r (1 - e^{-sT})^{p+r} \quad \text{2.33a}$$

$$= \frac{1}{s} \sum_{r=0}^{p} (1 - e^{-sT})^r \left[\frac{r!\, (1 - e^{-sT})}{(Ts)^r} - e^{-sT} \sum_{j=0}^{r-1} \frac{r!}{(r-j)!\, (Ts)^j} \right]$$

$$+ \frac{1}{s} \left[\frac{p!\, (1 - e^{-sT})}{(Ts)^p} - e^{-sT} \sum_{j=0}^{p-1} \frac{p!}{(p-j)!\, (Ts)^j} \right] \sum_{r=1}^{q} R_r\, (1-e^{-sT})^{p+r} \quad \text{2.33b}$$

Noting the form of the summation in 2.33b, a new polynomial may be

defined by:

$$H_m^r = \sum_{j=0}^{m-r} \frac{m!}{(m-j)!\,(Ts)^j} \qquad m > r$$

$$= 1 \qquad m = r \qquad \text{.... 2.34}$$

$$= 0 \qquad m < r$$

From this definition, we may show that

$$(1 - e^{-sT})\, r!/(Ts)^r - e^{-sT} H_r^1 = (1 - e^{-sT})\, H_r^o - H_r^1 \qquad \text{.... 2.35}$$

Using these polynomials and relation 2.35, the filter transfer function becomes:

$$G_{p,q}(s) = s^{-1} \sum_{r=0}^{p} (1 - e^{-sT})^r \left[(1 - e^{-sT})\, H_r^o - H_r^1 \right] + s^{-1} \left[(1 - e^{-sT}) H_p^o - H_p^1 \right] \sum_{r=1}^{q} R_r (1 - e^{-sT})^{p+r} \qquad \text{.... 2.36}$$

If the rank of the hold circuit is zero (q = 0), we have the relation

$$G_{p,0}(s) = s^{-1} \sum_{r=0}^{p} (1 - e^{-sT})^r \left[(1 - e^{-sT})\, H_r^o - H_r^1 \right] \qquad \text{.... 2.37}$$

Substituting $x = 1 - e^{-sT}$, this becomes

$$G_{p,0}(s) = x/s \left\{ \sum_{r=0}^{p} x^r H_r^o - \sum_{r=0}^{p} x^{r-1} H_r^1 \right\} \qquad \text{.... 2.38a}$$

In the second sum put m = r - 1, noting $H_o^1 = 0$:

$$G_{p,0}(s) = x/s \left\{ \sum_{m=0}^{p} x^m H_m^o - \sum_{m=0}^{p-1} x^m H_{m+1}^1 \right\} \qquad \text{.... 2.38b}$$

$$= x/s \left\{ x^p H_p^o - \sum_{m=0}^{p-1} x^m \left(H_{m+1}^1 - H_m^o \right) \right\} \qquad \text{.... 2.38c}$$

Again, defining new polynomials

$$P_m^r = H_{m+1}^{r+1} - H_m^r = \sum_{j=0}^{m-r} \frac{j\, m!}{(m+1-j)!\,(Ts)^j} \qquad \text{.... 2.39}$$

the transfer function for a (p,0) hold circuit becomes:

$$G_{p,0}(s) = s^{-1}(1 - e^{-sT}) \left\{ (1 - e^{-sT})^p H_p^o - \sum_{m=0}^{p-1} P_m^o (1 - e^{-sT})^m \right\} \qquad \text{.... 2.40}$$

And the transfer function for a (p,q) hold circuit is

$$G_{p,q}(s) = G_{p,0}(s) + s^{-1} \left[(1 - e^{-sT}) H_p^o - H_p^1 \right] \sum_{j=1}^{q} R_j (1 - e^{-sT})^{p+j} \qquad \text{.... 2.41}$$

where $G_{p,0}(s)$ is the transfer function defined in equation 2.40

H_m^r are the polynomials defined in equation 2.34

P_m^r are the polynomials defined in equation 2.39.

R_j are constants called rank coefficients.

The H_m^r and P_m^r polynomials defined above do not appear to have been previously reported in the literature, at least not in connection with sampled-data systems. The values of the first few polynomials as well as certain recurrence relations will be found in Appendix I. The final form of the filter transfer function is greatly simplified by the use of these polynomials.

As a check on equation 2.40, this expression should reduce to that in 2.3 and 2.15 for the zero and first order holds, respectively. For the conventional zero-order hold, p = 0 and q = 0, hence the transfer function of the filter is:

$$G_{0,0}(s) = s^{-1}(1 - e^{-sT})\, H_o^o \qquad \ldots\ 2.42$$

as $H_o^o = 1$, this expression agrees with that in equation 2.3. For the first-order hold, p = 1, and q = 0, hence the transfer function is

$$G_{1,0}(s) = s^{-1}(1 - e^{-sT})\left[(1 - e^{-sT})\, H_1^o - P_o^o\right] \qquad \ldots\ 2.43a$$

Substituting $H_1^o = 1 + (Ts)^{-1}$; $P_o^o = 0$, this expression reduces to

$$G_{1,0}(s) = (1 - e^{-sT})^2 \left[1/s + 1/(Ts^2)\right] \qquad \ldots\ 2.43b$$

which agrees with equation 2.15.

Examining the H_m^r and P_m^r polynomials, it is seen that these are rational functions of s. Furthermore, terms of the form e^{-ksT} may be treated as shown in equation 2.11 if k is an integer. Therefore, the modified Z-transform of $G_{p,q}(s)$ is

$$Z_m\left[G_{p,q}(s)\right] = G_{p,q}(z,m) = Z_m\left[G_{p,0}(s)\right] + (z-1)/z\; Z_m\left[H_p^o/s\right] \sum_{j=1}^{q} R_j \left(\frac{z-1}{z}\right)^{p+j} - Z_m\left[H_p^1/s\right] \sum_{j=1}^{q} R_j \left(\frac{z-1}{z}\right)^{p+j} \qquad \ldots\ 2.44$$

where $Z_m\left[F(s)\right]$ is the modified Z-transform of F(s). If the filter is

followed by a plant with known transfer function, the modified Z-transform is evaluated by a method similar to that used in equation 2.16. The modified Z-transforms for certain of the H and P polynomials will be found in Appendix I.

An examination of equations 2.40 and 2.41 reveals that the (p,q) hold circuits do not have a continuous impulse response so, in general, the output from such a filter will have finite discontinuities at the sampling instants. This may be partially corrected by placing a resistor-capacitor integrating network after the hold circuit. Such an integrating circuit has a transfer function of the form $(s + a)^{-1}$, so the overall system will have a continuous impulse response. The response of this system may be determined by considering the integrator as the plant in a sampled-data network and evaluating the modified Z-transform as shown in Section 2.3.

2.7 Analysis of the Error in a (p,q) Filter Output

The continuous input function (f)t, may be expanded in a Taylor's series about the point nT, as shown:

$$f(t) = f(nT) + Df(nT)\ (t - nT) + \ldots + \frac{D^r f(nT)}{r!}\ (t - nT)^r + \ldots . \quad 2.45$$

where D is the differential operator defined by the equation

$$Df(nT) = \left.\frac{df(t)}{dt}\right|_{t = nT}$$

The operator D may be expressed symbolically in terms of the ascending difference operator Δ:[30]

$$D = -T^{-1} \ln(1 - \Delta) = T^{-1}(\Delta + \Delta^2/2 + \Delta^3/3 + \ldots) \quad .... \quad 2.46$$

Substituting 2.46 in 2.45,

$$f(t) = f(nT) + \frac{(t - nT)}{T}\ (\Delta f(nT) + \frac{\Delta^2 f(nT)}{2} + \ldots) + \ldots \quad .... \quad 2.47a$$

Using the symbol $\delta_n^p = \Delta^p f(nT)$ this becomes:

$$f(t) = f(nT) + (\delta_n^1 + \delta_n^2/2 + ..)\frac{(t - nT)}{T} + (\delta_n^2 + \delta_n^3 + ..)\frac{(t - nT)^2}{2!\ T^2} \quad .... \ 2.47b$$

Comparing equations 2.47b and 2.45, we see that the (p,q) hold circuit approximates the continuous input function f(t) by using an expansion similar to 2.47b, but keeping only the first term in the series associated with $(t - nT)^r/T^r$ after multiplication by r!. If the rank of the filter is not zero, the series associated with $(t - nT)^r/T^r$ may be made to agree with the corresponding series in equation 2.47b by a suitable choice of the rank coefficients. This series will terminate at the δ^{p+q} term due to the finite memory of the filter. A hold circuit that uses only the lowest difference appearing in each δ_n^r series in equation 2.47b, except possibly in the series starting with the term δ_n^p, will be called a Group I hold circuit.

If the continuous input may be approximated by a polynomial whose degree does not exceed p+q then the Group I hold circuit output will coincide with the continuous function at the beginning and end of each sampling interval when the rank coefficients are all equal to unity. This may be demonstrated by the following argument: at the beginning of each sampling interval, the hold circuit output is f(nT), which coincides with the continuous function at that instant; taking the limit of equation 2.25 as $t \to (n+1)T$ and setting all $R_i = 1$, we get:

$$\lim_{t \to (n+1)T} f_h(t) = f(nT) + \delta_n^1 + \delta_n^2 + \ldots + \delta_n^{p+q} \quad .... \ 2.48$$

From equation 2.19 $f\left[(n+1)T\right] = Ef(nT)$, and by equation 2.21, E may be replaced by the expression

$$E = (1 - \Delta)^{-1} \quad .... \ 2.49a$$

which, by the binomial theorem becomes

$$E = \sum_{n=0}^{\infty} \Delta^n \quad .... \ 2.49b$$

Therefore,

$$f\left[(n+1)T\right] = \sum_{n=0}^{\infty} \Delta^n f(nT) \quad .... \ 2.50a$$

$$= \sum_{p=0}^{\infty} \delta_n^p \qquad \text{.... 2.50b}$$

$$= f(nT) + \delta_n^1 + \delta_n^2 + \ldots \qquad \text{.... 2.50c}$$

This series will terminate at δ_n^r if f(t) is a polynomial of degree r.[30] Therefore, if $r \leqslant p+q$, expressions 2.48 and 2.50c are identical and the hold circuit output coincides with f(t) at the end of the sampling interval.

The error, or difference, between the continuous input and the filter output, may be determined by subtracting equation 2.25 from equation 2.47b. The design of the hold circuit may be so modified as to minimize this error by including as many differences as its memory allows in each δ_n^r series in equation 2.47b. Such a hold circuit may be described by only one parameter, its memory size, and will be called a Group II hold circuit.

Both the Group I and Group II hold circuits have discontinuous impulse responses due to the constant term, f(nT), in the series expansions for their outputs. This discontinuity at the sampling instants may be removed by the same method used by Porter and Stoneman to overcome this problem. The filter circuitry is so modified that the last sample, f(nT), is integrated before being applied to the output. Such a hold circuit will be called a Group III circuit, and its output will have the form:

$$f_h(t) = f(nT)(t - nT)/T + K_1(t-nT)/T + K_2(t-nT)^2/T^2 + \ldots \qquad \text{.... 2.51}$$

A Group III hold circuit may be made to fit an arbitrary continuous function, with the same accuracy as the Porter-Stoneman system, although the filter configuration will be quite different.

The transfer functions for a Group II and Group III hold circuit may be determined by an analysis similar to that given for the Group I hold, and this problem will be left for a future investigation.

The implementation of any of these hold circuits requires the following components:

1) A resetable memory with sufficient capacity to store the values of p+q+1 samples,
2) Integrators and summers to generate the desired polynomial output from these sample values.

The experimental work, described in the following chapters, investigates the suitability of analog computer operational amplifiers[32] to perform all these functions. A simple hold circuit is tested by comparing its performance with that predicted by Z-transform analysis. Discrepancies between the two values are a measure of the suitability of this simulation scheme for this task. The design of more complex hold circuits is described.

CHAPTER III

THE SIMULATION AND TESTING OF A FINITE-MEMORY HOLD CIRCUIT

The preceding analysis has suggested a method of simulating an operational hold circuit on an analog computer. The components which are necessary for the implementation of this scheme are resetable memory units, a sampler and suitable testing facilities. These are described in this chapter.

3.1 Simulation of the Hold-Circuit Memory

The memory units must store the value of the samples as they are received and supply these quantities as constant-level outputs to the associated circuitry. A (p,q) hold circuit will contain p+q+1 such units, so each one must be capable of storing its sample value for D = (p+q+1)T seconds, where T is the sampling interval.

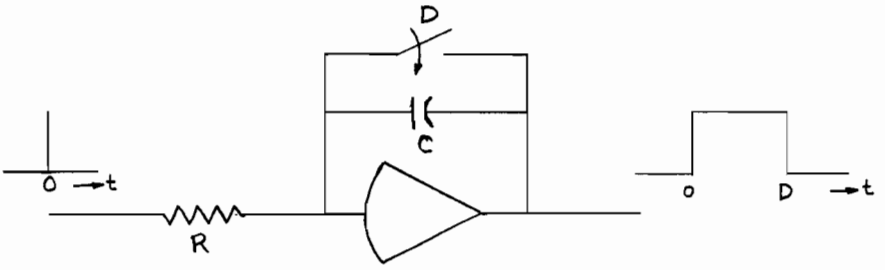

Figure 3.1

The basic hold circuit memory unit.

A simple circuit to accomplish the necessary storage is shown in Figure 3.1. In this circuit, an operational amplifier is used as an integrator to convert the sample impulse input into a step output. The magnitude of the output step is determined by the charge on the feedback capacitor and is proportional to the area under the input pulse. The ratio of sampling pulse width to the integrator time constant is the

scaling factor which relates the magnitude of the memory output to the sample height. For very narrow pulse widths, it will be difficult to make this ratio equal to unity. A commutator switch is synchronized with the sampler to discharge the feedback capacitor every $D = (p+q+1)T$ seconds. For an impulse input, the transfer function for this unit is $(1 - e^{-sD})/s$.

The feedback capacitor must have a very low leakage conductance to retain a constant charge on its plates for the necessary length of time. The D-C drift in the operational amplifier must be negligible or it will alter the output voltage of the unit. Any circuitry connected to the memory unit during the interval between successive pulse storages must not have any signal associated with it. The performance of an experimental memory unit is described in Chapter IV.

3.2 Analog Computer Connections for Hold Circuit Simulation.

The output of an operational amplifier is always inverted with respect to its input and this fact makes these devices suitable for computing the various differences required to generate a particular polynomial. The determination of the analog computer connections is facilitated by the scheme described in Appendix II. This scheme requires $p(p+1)/2$ integrators with associated commutator switches to simulate a (p,q) hold circuit, exclusive of the ones used in the memory. In addition to these integrators, $p/2$ or $(p-1)/2$ (whichever is an integer) inverters and a number of summers are also required. The method of calculating the scaling factors at the summer inputs is also shown in Appendix II.

The scheme has been applied to the design of a $(3,2)$ hold circuit with all rank coefficients equal to unity, and the result is

shown in Figure 3.2. In this figure, the symbol M_r denotes the memory unit which stores the sample whose value is $f\left[(n-r)T\right]$. Commutator switches are not shown in Figure 3.2, but every integrator in the main computer has one connected across its feedback capacitor to discharge this at the end of each sampling interval.

The memory of the hold circuit will contain p+q+1 storage units, and some means must be found to switch these into the correct M_r position at the start of each sampling interval. The following method could be used to accomplish this. Immediately before a sample is received, the main computer is reset and disconnected from the memory bank. The memory unit in the M_{p+q} position is reset by discharging its feedback capacitor and then switched to the M_0 position, all other memory units being advanced to the next higher position. The sample is then received and applied to the unit in the M_0 position, whereupon the memory bank is reconnected to the main computer. The details of this switching sequence for a two-unit memory are shown in Figure 3.3.

If the scaling factor for the memory units is equal to k, the filter may be adjusted to have an overall scale factor of unity by multiplying the inputs to the final summer in the main computer by the factor 1/k. The performance requirements for the integrators in the main computer are the same as for those in the memory.

3.3 Facilities for Testing Sampled-Data Systems.

In building up the laboratory facilities for the study of finite memory hold circuits, apparatus was built or purchased which would also be suitable for the study of other sampled-data systems. Because control systems are basically low-frequency devices, the apparatus adopted has a frequency range extending from a fraction of a cycle per second into the

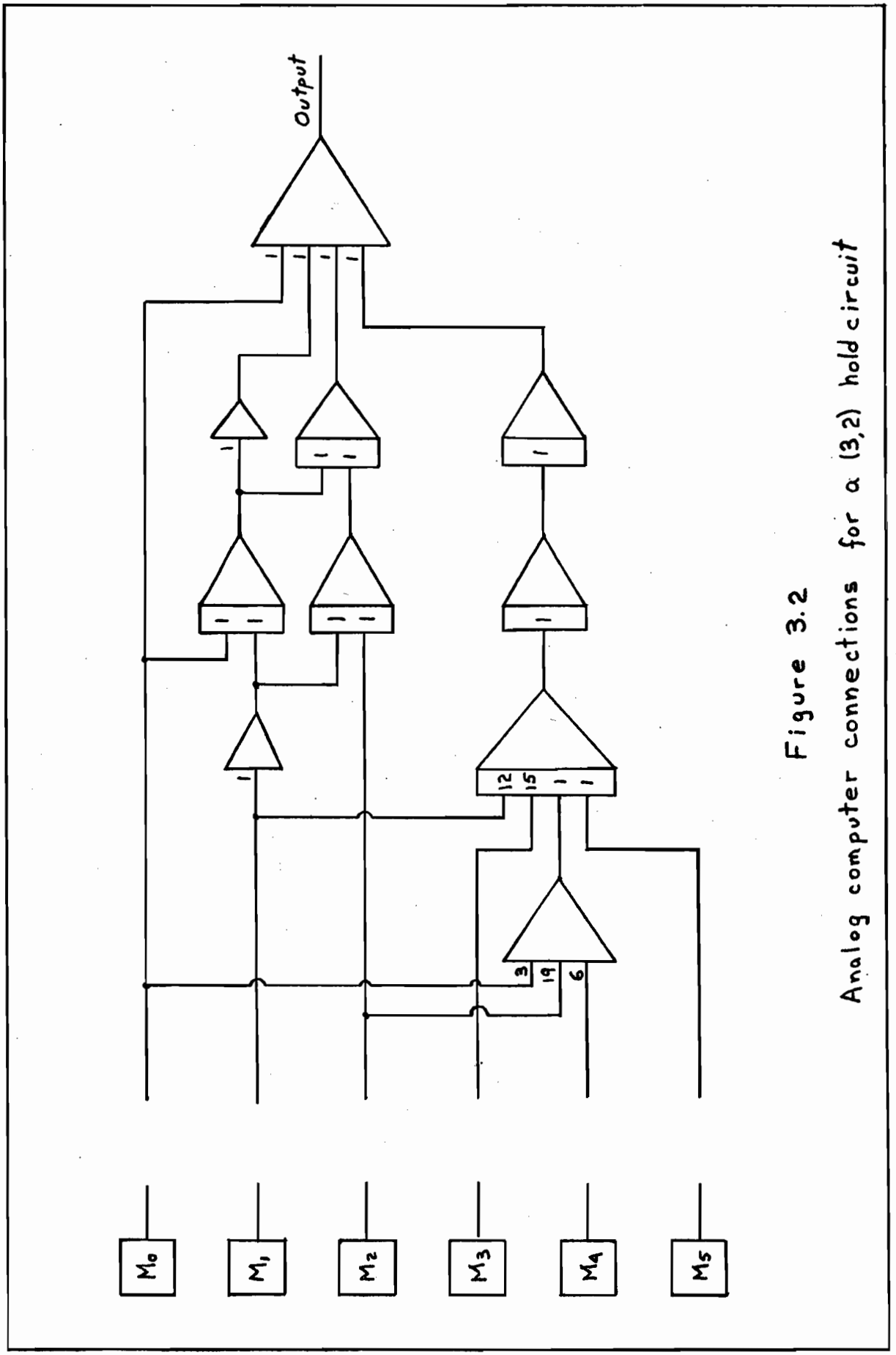

Figure 3.2

Analog computer connections for a (3,2) hold circuit

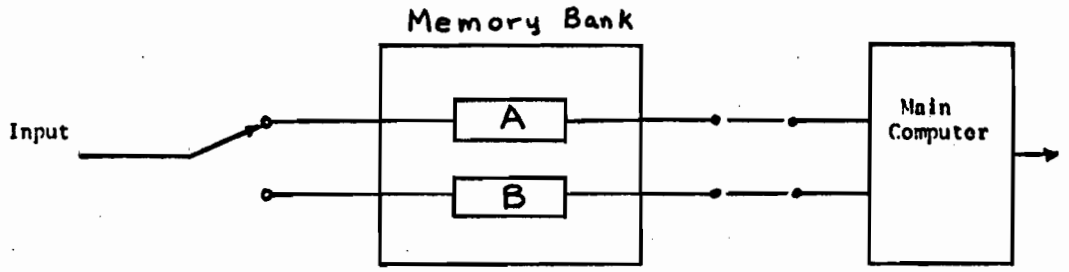

Configuration after last switching

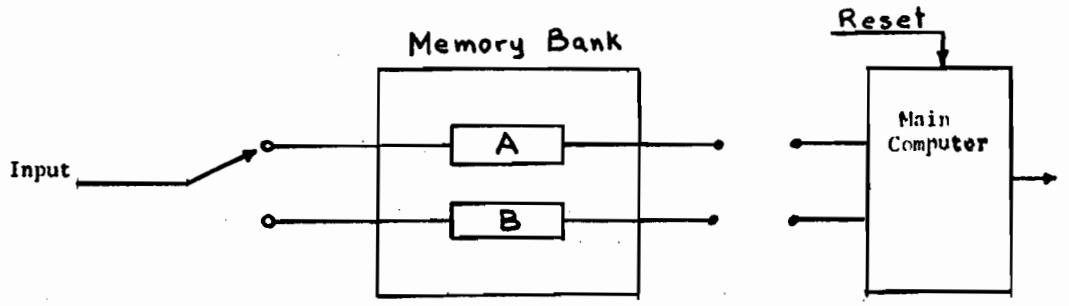

Memory bank is disconnected and computer is reset

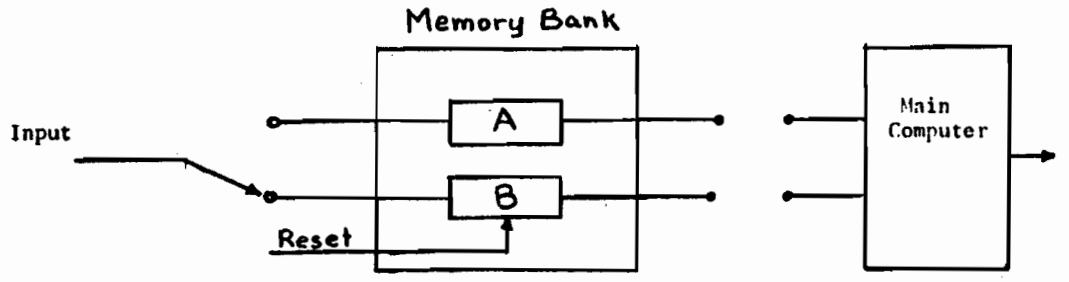

M_1 memory unit is reset and switched to M_0 position

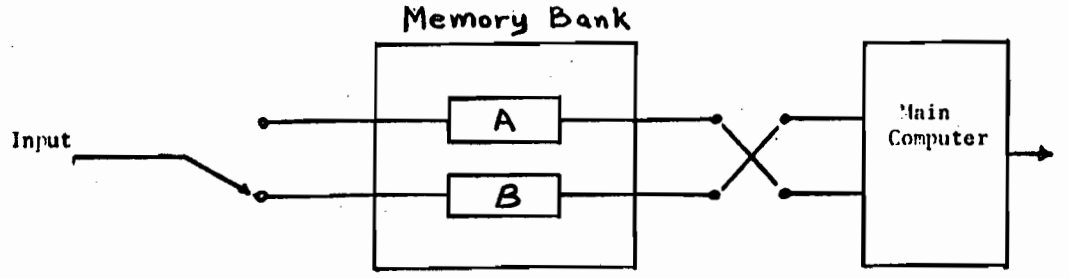

Sample is received and memory bank is reconnected

Figure 3.3
Switching Sequence

audio frequencies. A block diagram of the apparatus connections is shown in Figure 3.4.

The function generator is a Krohn-Hite Model 440 push-button oscillator. Its frequency range is continuously adjustable from 0.001 cps to 100 Kc. Sine waves with amplitude variable up to 10 volts rms on open circuit, and square waves with a fixed amplitude of 10 volts p-p on open circuit are available. Other periodic waveforms may be generated by using an analog computer to integrate the square wave output.

The sampling pulse train is generated using the Tektronix 160-Series pulse and waveform generators. These units are capable of supplying pulses of either polarity with amplitude continuously variable from 0 to 50 volts. The pulse width may be varied continuously from 1 μsec. to 10 sec. The pulse spacing is variable from 100 μsec. to 10 sec., and the pulse may be delayed by any amount over a repetition period relative to some trigger signal.

The low-pass filter is used to study the effect of combined hold circuit restoration and low-pass filtering. Two units are available, for either band-rejection or band-pass characteristics. The band-rejection filter is a Krohn-Hite Model 350-A, and the band-pass filter is a Krohn-Hite Model 330-A. The high and low frequency cut-offs of both filters may be tuned independently from 0.02 cps to 2Kc.

A Donner Model 3000 analog computer is used in the simulation of hold-circuits. This computer has ten operational amplifiers with no chopper stabilization. The individual amplifiers have an open-loop gain of 3×10^4 under a load of 20 Kohms, over most of their operating range, and saturate when their output voltage reaches ± 100 volts. The bandwidth of these amplifiers extends well into the audio frequencies, and

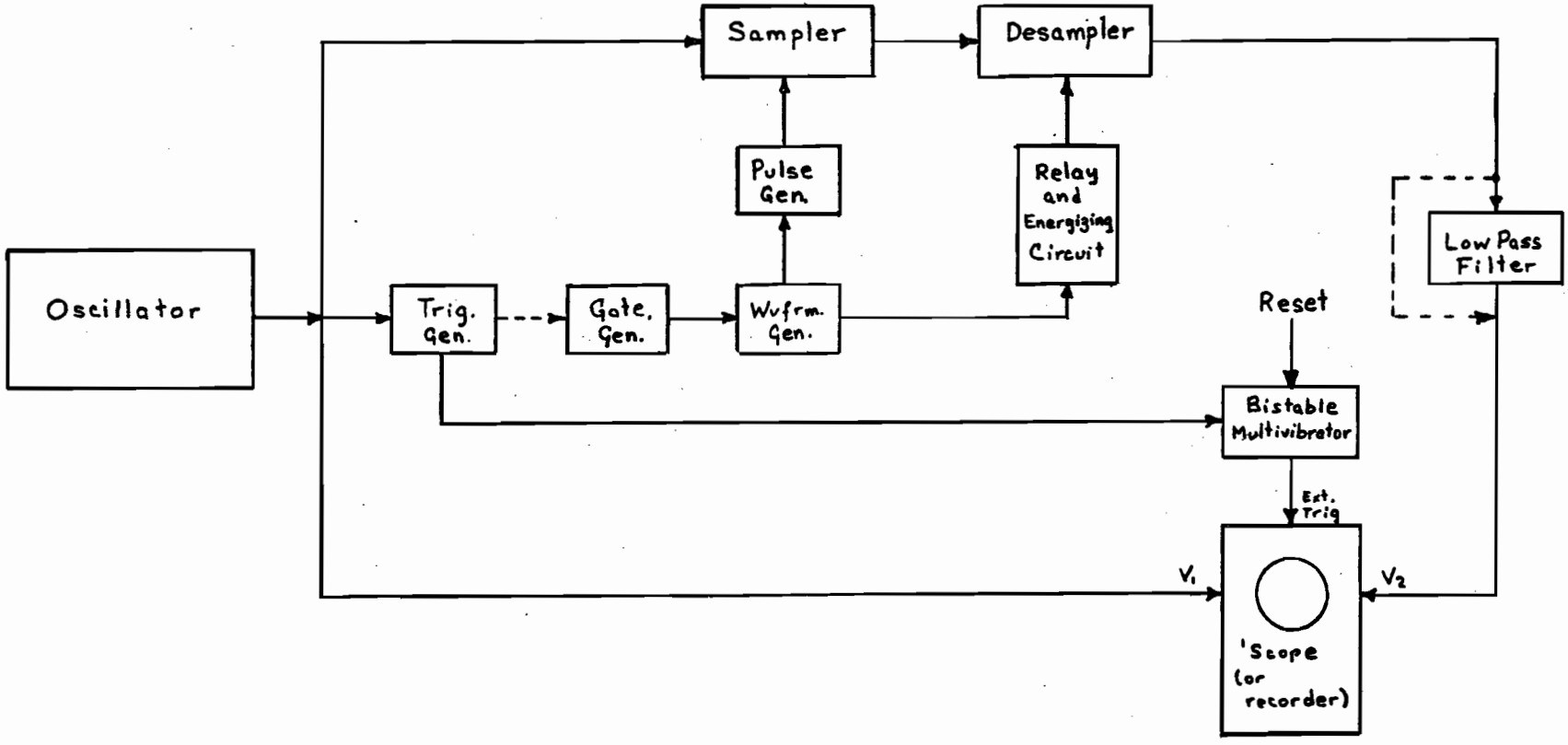

Figure 3.4

Apparatus Block Diagram

their short-term random drift after warm-up is only about 0.5 mVolt - referred to the amplifier input.

Several read-out devices are employed in the testing of sampled-data systems. These are: a Tektronix Model 502 dual-beam oscilloscope equipped with a Dumont camera, a Sandborn Model 152 two-channel recorder with associated preamplifiers, and a Moseley Model 2D x-y recorder.

The remaining apparatus was specially built for this research and each unit is described separately below. A photograph of the laboratory arrangement is shown in Figure 3.5.

3.4 The Electronic Sampler

The sampling operation may be accomplished either by mechanical or electronic switches. Mechanical switches have the advantage that their open-circuit resistance is several orders of magnitude higher than the corresponding quantity in an electronic sampler, likewise their short-circuit resistance is several orders of magnitude lower than that of an electronic switch. Also, direct-coupled electronic switches may introduce a random drift in their output. In spite of these limitations of electronic switches, they were adopted in this research because they are capable of faster switching speeds than mechanical switches, and it was desirable to build as flexible a simulation scheme as possible.

The sampling operation may be regarded as the balanced modulation of a pulse train by the input signal. A circuit which can be used as a balanced modulator[33] is shown in Figure 3.6. This basic circuit was considerably improved to meet the problem at hand and the electronic sampler which was developed is shown in Figure 3.7.

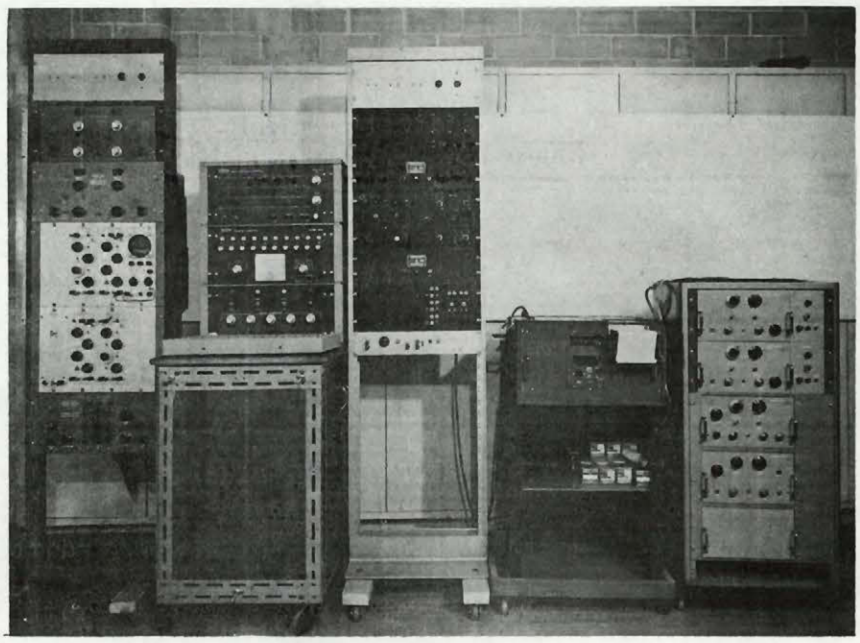

Figure. 3.5

Experimental simulation and testing facilities.

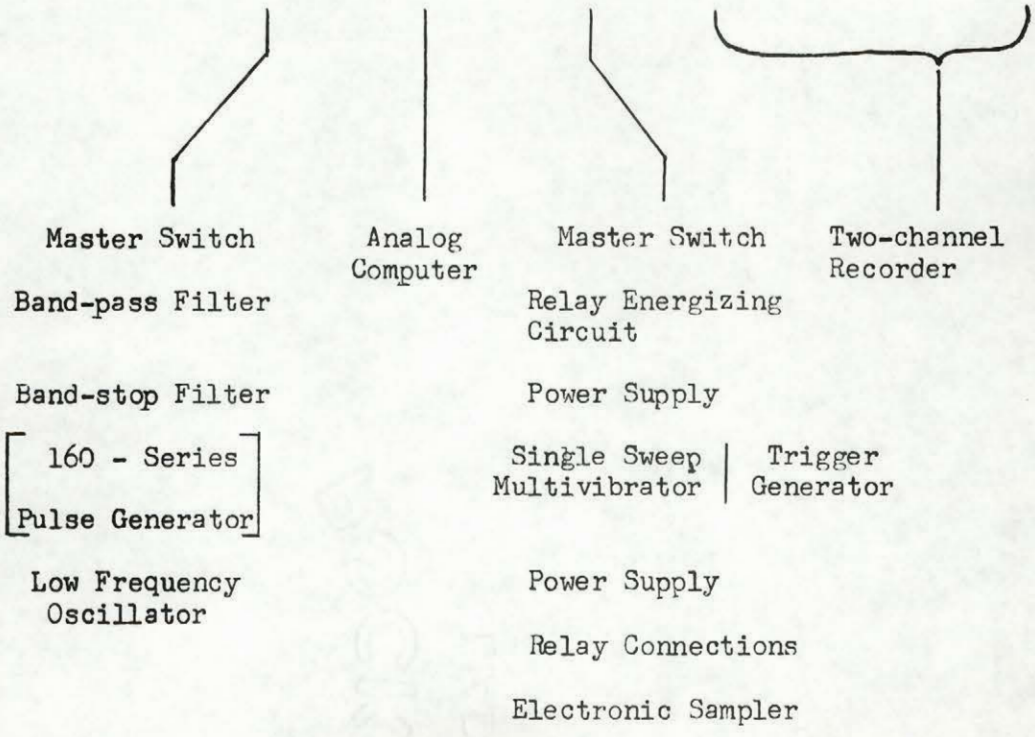

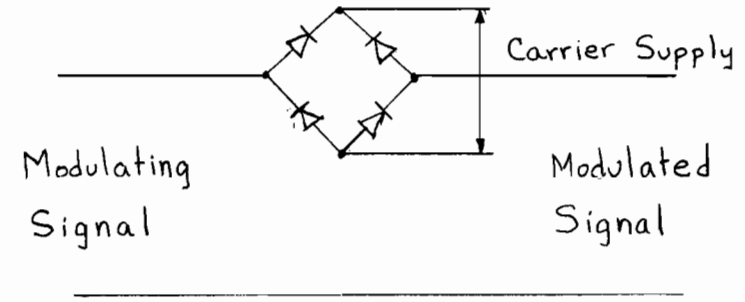

Figure 3.6
A diode modulator circuit

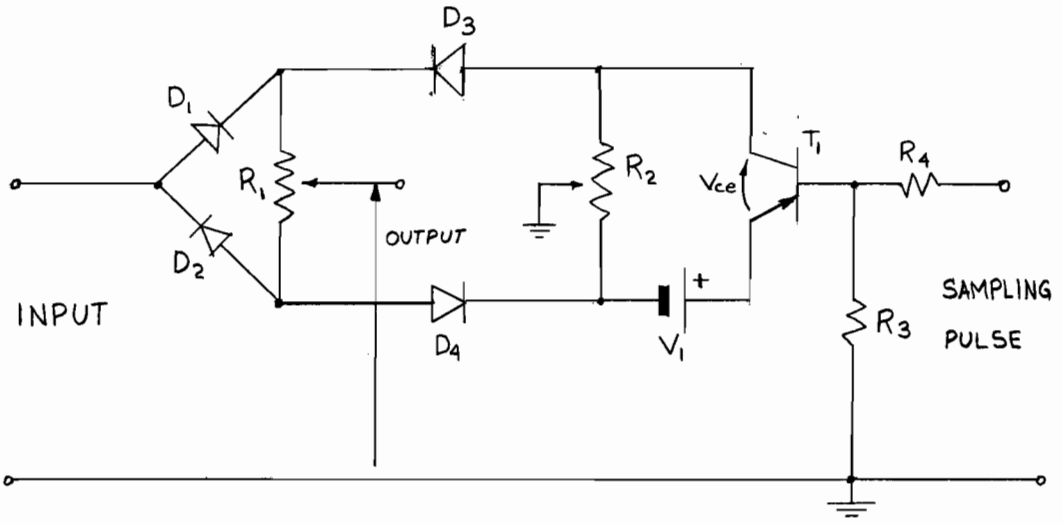

Figure 3.7
The electronic sampler.

The circuit parameters of the electronic sampler are so chosen that a large collector current flows in the transistor when no signal is present at the pulse input terminals. This collector current is divided between the two parallel paths containing R_1 and R_2. R_1 is made much larger than R_2 so that most of this current flows in the latter. The centre-tap of R_2 is adjusted until the voltages on either side of it have the same magnitude. The centre-tap of R_1 is then set to the point on this potentiometer which is a ground potential. R_4 is a large resistance used as a buffer between the sampler and the pulse generator.

When R_1 and R_2 have been set to their proper positions, the junction of diodes D_1 and D_3 is at a potential of $E = (V_1+V_{ce})/2$ above ground, and the junction of diodes D_2 and D_4 is at the same potential below ground. Thus, diodes D_1 and D_2 are open-circuited to any input signal whose amplitude is less than E, and the sampler output is zero for all such voltages. To sample a signal, a positive pulse with an amplitude large enough to bias the transistor to cut-off is applied at the sampling pulse input terminals. No current flows in potentiometer R_1 under these circumstances and any input signal appears, slightly attenuated, at the sampler output.

The diodes and transistor used in the experimental sampler were not selected with any particular care, components which were on hand being used. The component values which were used are the following:

D_1, D_2		OA85	(National)
D_3		MA303	"
D_4		MA301	"
T_1	pnp	23B170	"
R_1, R_3, R_4		10 Kohms	
R_2		2 Kohms	
V_1		9 Volt battery	

With these component values, the transfer characteristics for the sampler in its "ON" and "OFF" states are shown in Figures 3.8a and 3.8b, respectively. The transfer characteristic in the conducting state is seen to have a non-linearity at the origin when the sampler output is open-circuited. This is due to the non-linear characteristics of the diodes. This non-linearity is markedly reduced when a 10 Kohm

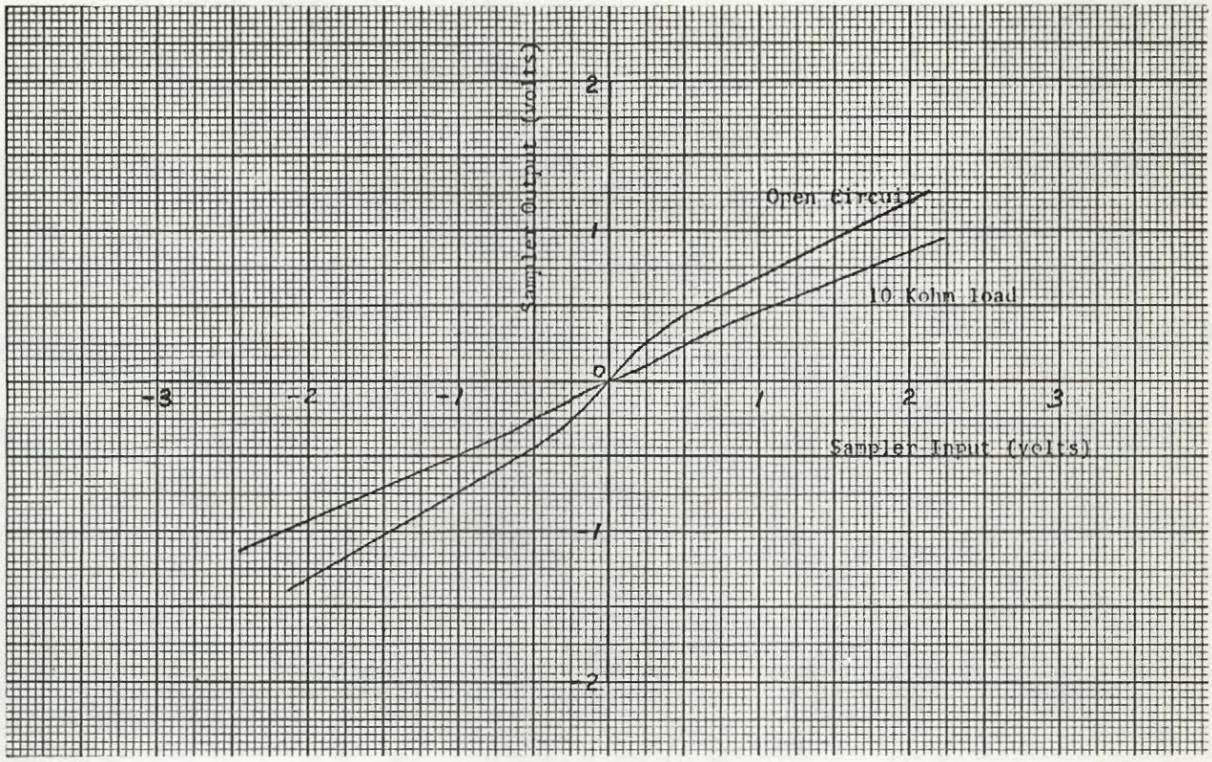

Figure 3.8a
Transfer Characteristics with
Diodes Closed

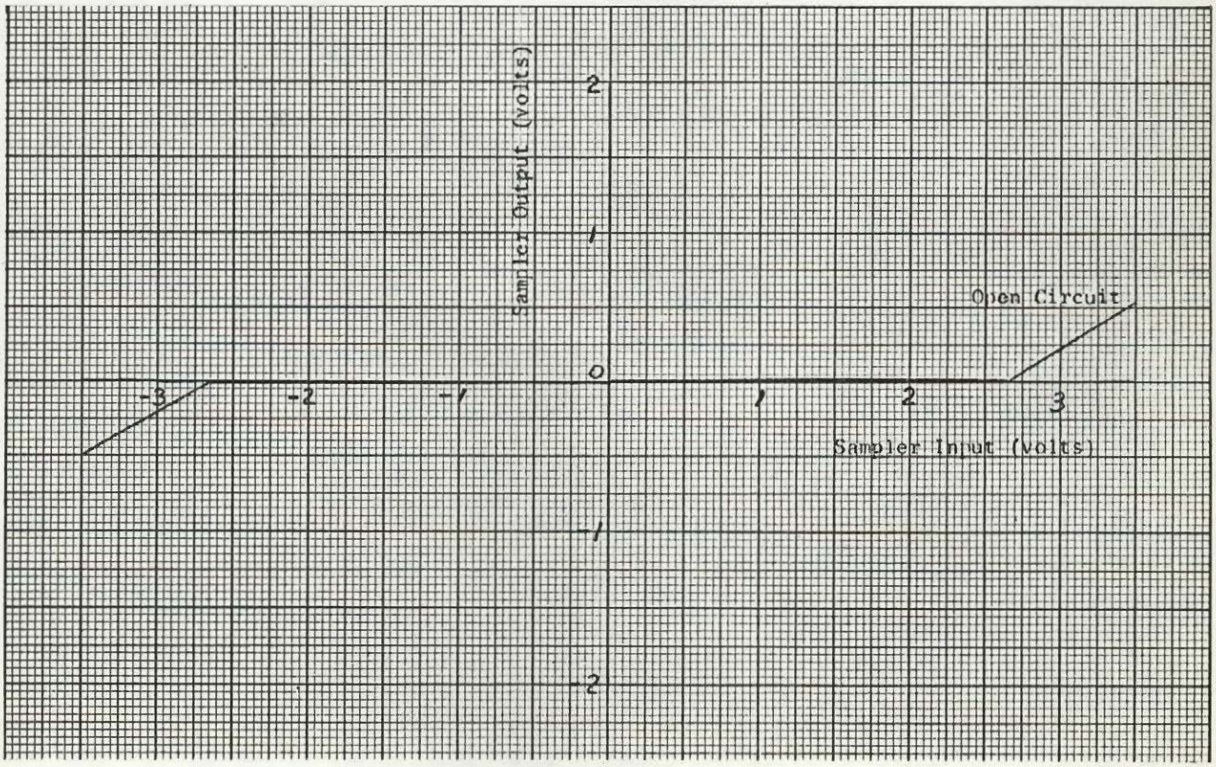

Figure 3.8b
Transfer Characteristics with
Diodes Open

load is placed across the sampler output terminals, and the sampler is operated with such a load in practice. In its conducting state, with a 10 Kohm load, the magnitude of the sampler transfer function is 0.45. This could be corrected by placing a direct-coupled amplifier with a gain of 1/0.45 after the sampler, but this was not done. The sampler transfer characteristic shows no appreciable phase shift for input frequencies up to 3 Kc, and the phase shift does not become serious for frequencies below 10 Kc. This phase shift is largest at low input signal levels, and seems to be due to the semi-conductor properties of the diodes.

Figure 3.8b shows that the sampler will operate satisfactorily with input signals whose amplitude does not exceed 2.5 volts. This limit could be increased by increasing the size of the battery, V_1. The effect of a misadjustment of R_2 on these curves is to shift them relative to the y-axis, while a misadjustment of R_1 shifts them relative to the x-axis. Furthermore, if R_1 is not set exactly in its centre position, the curves in Figure 3.8a will not be symmetrical about the origin.

The open circuit transfer characteristic suggests another application for the electronic sampler. It could be used as a dead-zone simulator in the study of control-systems. The magnitude of the dead-zone may be varied by changing V_1, and the slope of the extremities may be adjusted by placing a variable-gain amplifier after the sampler.

The sampler which was built has operated successfully with sampling pulses as narrow as 5 μsec. and pulse intervals as short as 100 μsec. The apparatus available did not permit testing the sampler with shorter pulse intervals.

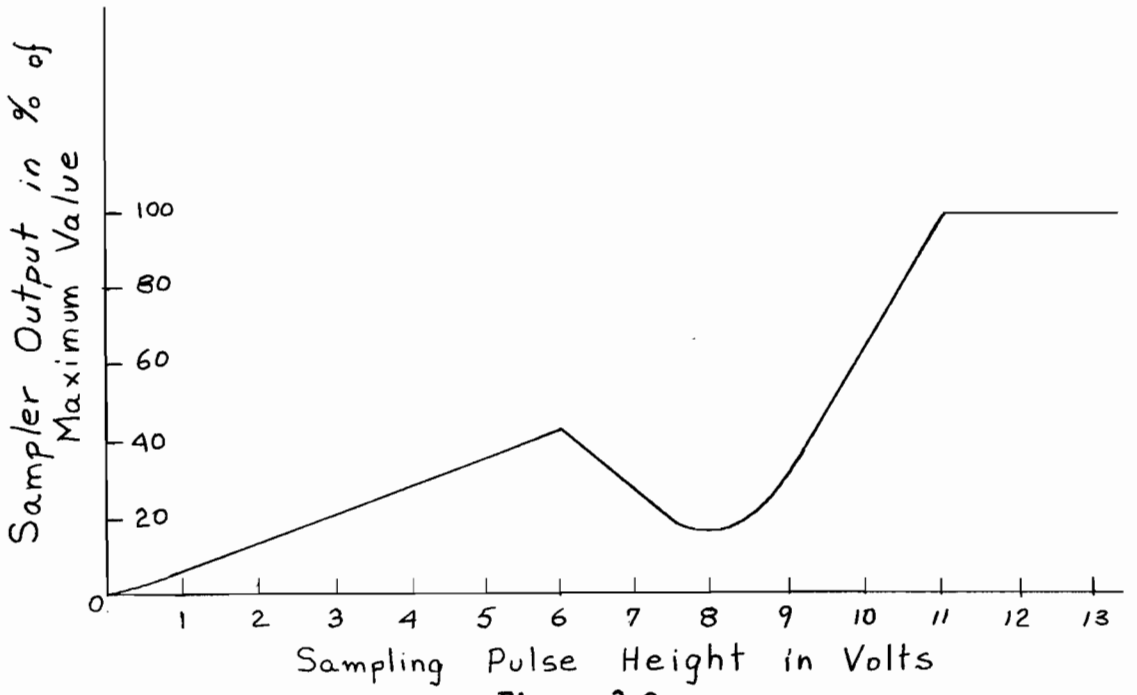

Figure 3.9

Dependence of sampler output on sampling pulse height.

The dependence of the sampler output on the sampling pulse height is shown in Figure 3.9. The shape of this curve depends on the setting of potentiometers R_1 and R_2, but these do not affect the value of the pulse height at which the sampler output reaches its maximum value. Thus, the sampler output is independent of the sampling pulse height if the latter exceeds 11 Volts, a value which is well within the range of the 160-Series pulse generator. The reverse collector leakage current[34] in T_1 should be small or it will develop a voltage across the upper half of R_2 which will appear at the sampler output when the transistor is cut-off.

An examination of the sampler circuit in Figure 3.7 shows that the lower part of R_2 carries the total emitter current, I_e, while the upper part carries the total collector current, I_c. If R_2 has been adjusted correctly then

$$I_c R_c = I_e R_e \qquad \ldots\ 3.1$$

where R_c and R_e are the upper and lower halves of R_2, respectively. The total collector current is made up of two components, one of which is temperature dependent. This temperature dependent component is called the collector leakage current, I_{co}.[34] Any change in I_{co} will result in an unbalance of the two voltages in each half of R_2. The unbalance voltage will be denoted by V and is given by the expression

$$V = I_c R_c - I_e R_e \qquad \ldots. 3.2$$

The dependence of this quantity on I_{co} is

$$\frac{\Delta V}{\Delta I_{co}} = \frac{\Delta I_c}{\Delta I_{co}} R_c - \frac{\Delta I_e}{\Delta I_{co}} R_e \qquad \ldots. 3.3$$

When the appropriate expressions[34] are substituted in equation 3.4 we have the relation

$$\frac{\Delta V}{\Delta I_{co}} = \frac{R_c}{1-\alpha+\frac{\alpha R_e}{R_b+R_e}} - \frac{R_e}{1-\alpha+\frac{R_e}{R_b}} \qquad \ldots. 3.4$$

where R_b is the resistance in the base circuit

$\alpha = di_c/di_e$ is the forward current gain of the transistor in the common-base configuration.

For the circuit in Figure 3.7, these values are, approximately,

$$R_c = R_e = 1 \text{ Kohm}$$

$$R_b = 5 \text{ Kohm} \qquad \alpha = 0.99$$

Hence, equation 3.4 becomes:

$$\Delta V/\Delta I_{co} = 1 \text{ Kohm} \qquad \ldots. 3.5$$

Any changes in the V defined by equation 3.2 will result in a corresponding D-C unbalance in the sampler output, as the centre-tap of R_1 will no longer be at ground potential. The short-term random D-C unbalance at the sampler output, due to all causes, is shown in Figure 3.10. The smaller peaks have a typical magnitude of 1 — 2 mv.

Assuming these are due to changes in I_{co}, then the corresponding ΔI_{co} is 1 - 2 μamps. from equation 3.5. Variations of other transistor parameters, such as the base-to-emitter voltage, may also contribute to these peaks. The larger and more pronounced changes have a magnitude of about 7 - 8 mv. These changes were attributed to poor electrical contact between the wiper arm and the resistive surface, and it is recommended that high-quality multiturn potentiometers be used in future investigations.

Typical sampler outputs are shown in Figures 3.11a and 3.11b. The input signal is a 1 cps sine wave and the sampling interval is 0.1 sec. in both photographs. Figure 3.11a shows the output with a sampling pulse width of 2 msec., and the other figure shows the output with a pulse width of 20 msec. The vertical scales of all traces are the same.

3.5 Memory Circuit Resetting.

The proposed method of simulating finite memory hold circuits requires commutator switches, operating in synchronism with the sampler, to discharge the feedback capacitors in the various integrators at the end of each sampling interval. Again, either mechanical or electronic switching could be used, but it was decided, in this initial study, to sacrifice high speed operation for freedom from drift so relays were adopted for this purpose.

The particular relays selected were the Northern Electric Type 293 dry-reed relay. Their construction is illustrated in Figure 3.12. The contacts are made of a magnetic material which has been plated with a conductive surface. These are very light and small, so the relays are suitable for low-power, high-speed switching.

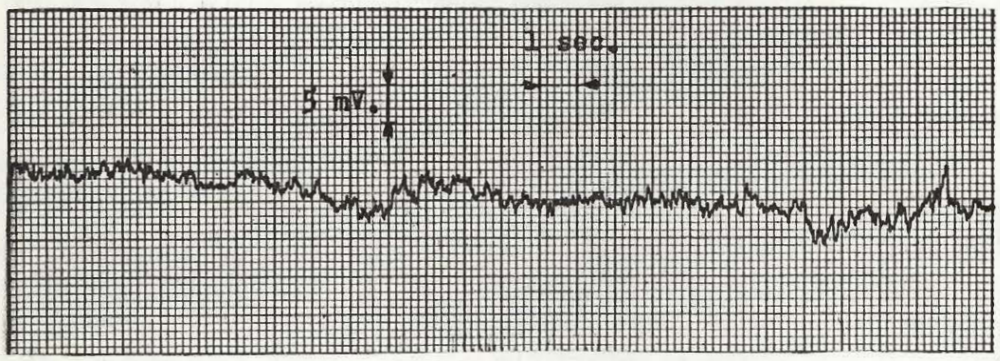

Figure 3.10

Short-term random D-C unbalance at the sampler output.

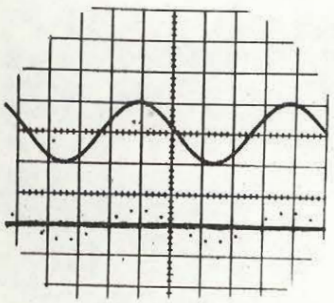

Figure 3.11a

Sampler output with
a 2 msec. pulse width

f(t) = 1 cps sine wave
T = 0.1 sec

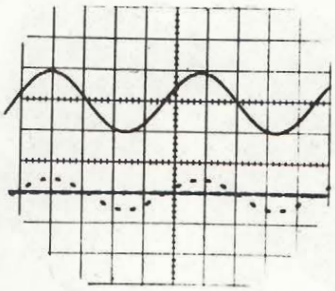

Figure 3.11b

Sampler output with
a 20 msec. pulse width

f(t) = 1 cps sine wave
T = 0.1 sec

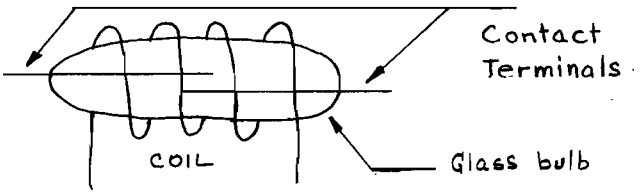

Figure 3.12

The construction of a dry-reed relay.

The particular relays used require a turn-on current of 6 mA. and a holding current of 2 mA. The circuit built to satisfy these requirements is shown in Figure 3.13. It comprises a monostable multivibrator with adjustable pulse width driving a cathode-follower with the relay coil in the cathode circuit. The basic design for the multivibrator is according to Chance et al.[35] The output pulse width is continuously variable from 1 msec. to 6 msec. The input triggering level requirements vary with the pulse width of the output, being about 25 volts for a 1 msec. pulse and decreasing approximately linearly to 5 volts for a 6 msec. pulse. The triggering pulse for this circuit is used as the reference for all other switching circuits, and the sampling pulse is delayed about 5 msec. behind this reference.

The characteristics of the Type 293 relay coil change with frequency and also depend on whether the contacts are open or closed, so an exact analysis of the optimum impedance of the generator which energizes the coil is virtually impossible. However, the following general observations may be made. Although the turn-on current is 6 mA., it is possible to close the relay contacts with a fast-rise 2 - 3 mA. pulse by taking advantage of the self-resonance of the coil. Therefore, the resonant frequency of the coil and generator impedance should be high enough for the coil current to reach its turn-on value in the

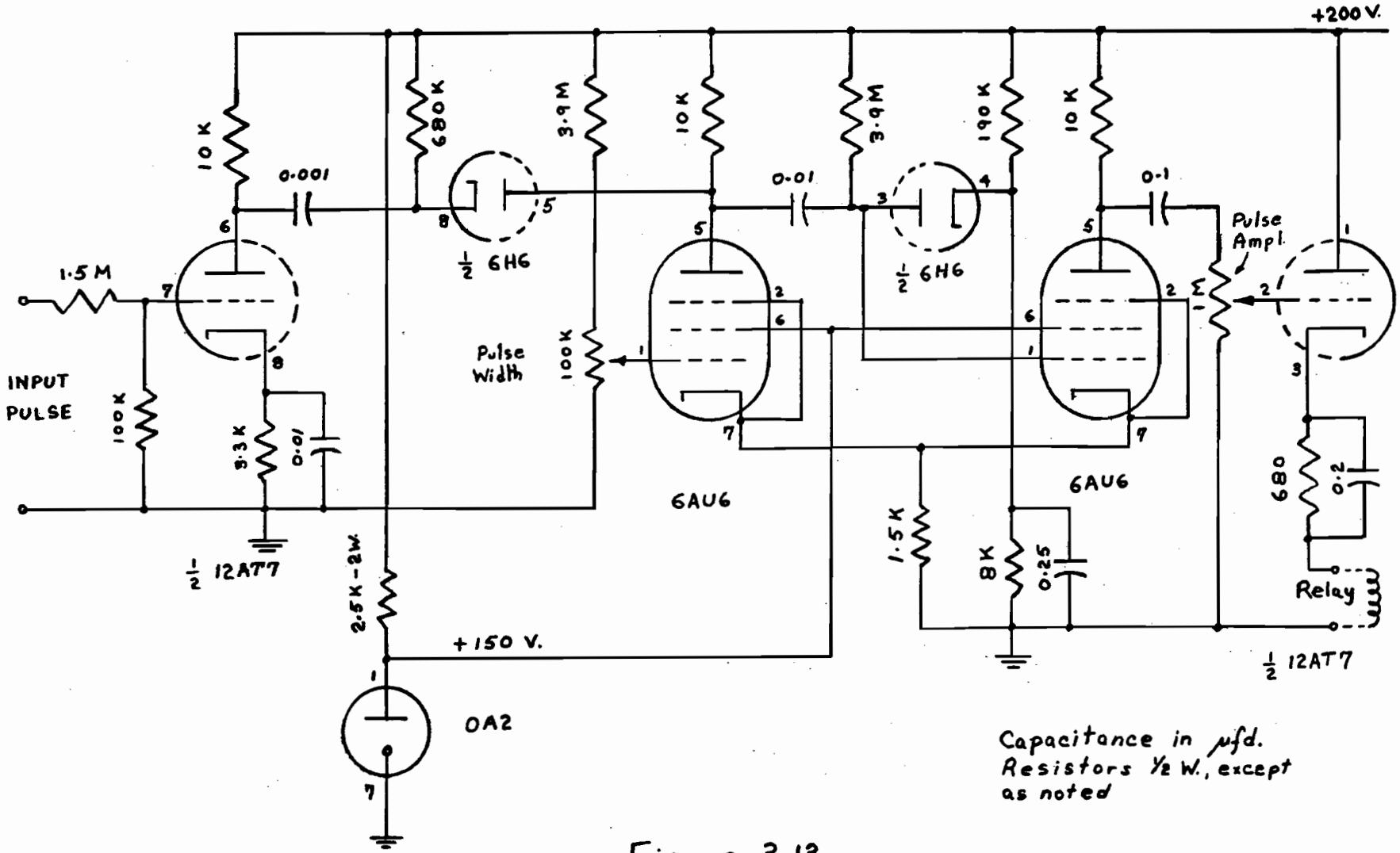

Figure 3.13
Relay Energising Circuit

shortest possible time. The damping in this circuit must be large enough to limit the amplitude of the resulting current oscillations to a value which will not cause a jitter of the relay contacts. The resistor-capacitor network shown in series with the relay coil in Figure 3.13, serves to adjust the generator impedance to a satisfactory value.

Figures 3.14a and 3.14b show the current and voltage in the relay coil after it has been energized by a 2 msec. pulse. The horizontal scales in both photographs are 2 msec./div. The vertical scale in Figure 3.14a is 2 mA/div and that in Figure 3.14b is 10 volts/div. The current waveform shows that there is about a 1 msec. delay after the coil is energized before the contacts close. The inductance of the coil suffers an abrupt change at this point which causes the discontinuity in the curve at the 6 mA. level. The energizing voltage is cut off after 2 msec. and the coil current begins to decay at this point. About 1 msec. after the end of the pulse, the coil current falls below the holding value, but the inertia of the contacts and their residual magnetism prevent these from opening immediately. The coil current rises to the holding value and then decays, the contacts finally opening about 4 msec. after the pulse has ended.

To protect the relay contacts from current surges which occur when discharging integrator capacitors, a 1 Kohm resistor is always connected in series with them. Figure 3.15 shows the voltage output of an integrator whose feedback capacitor is discharged with the Type 293 relay. The horizontal scale is 1 msec/div. The upper trace shows the integrator output, which remains at its original value for about 1 msec after the relay coil is energized, and then decays exponentially to zero in 0.5 msec. The remaining interval is the time taken by the relay

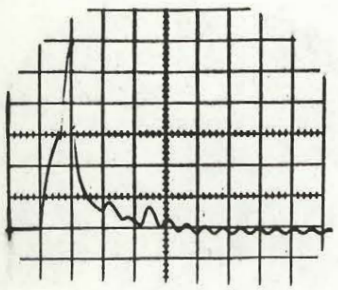

Figure 3.14a

Current through relay coil

Vert. Scale: 2 mA/div
Horiz. Scale: 2 msec/div

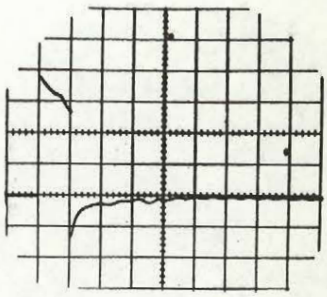

Figure 3.14b

Voltage across relay coil

Vert. Scale: 10 volts/div
Horiz. Scale: 2 msec/div

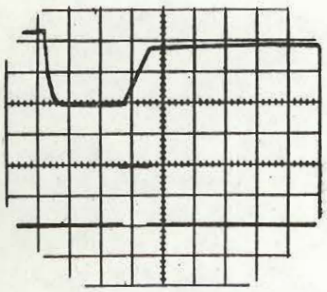

Figure 3.15

Integrator output during discharging cycle

Horiz. Scale: 1 msec/div

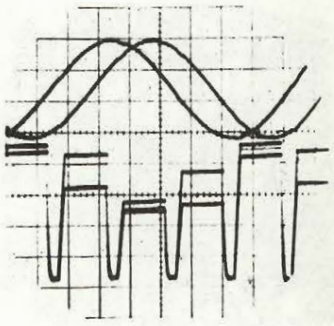

Figure 3.16

Double-exposure effect produced in photographing sampled-data signals.

contacts to re-open, and when this is completed the sampling pulse, shown in the lower trace, produces the ramp in the operational amplifier output. It is seen that the sampling pulse is delayed slightly less than 4 msec behind the energizing pulse, the complete discharging cycle taking 3 msec. From the performance of the coil with a 2 msec pulse it might be surmised that the discharging cycle would be longer; however, with shorter pulses, the coil current is not able to rise as far above its turn-on value and hence the oscillations following the first crossing of the holding value do not have sufficient amplitude to keep the contacts closed. Figure 3.15 was obtained using an energizing pulse of 1 msec, which seems to be the best performance obtainable with these relays.

3.6 Oscillographic Recording of Sampled-Data Signals.

The normal method of photographing an oscilloscope trace is to synchronize its sweep to the waveform being observed and then to expose the film for several sweeps. However, when a dual-beam oscilloscope with independent signals on the two channels is used, normal photographic techniques produce a double-exposure effect because the periods of the two signals are different. Figure 3.16 shows a photograph which was taken when the oscilloscope sweep was synchronized with the sampling pulses.

To produce photographs which can be interpreted unambiguously, a bistable multivibrator was constructed to generate single oscilloscope sweeps. The circuit of this multivibrator is shown in Figure 3.17. It is quite conventional[35] except for the input stage which is direct-coupled through a diode to one of the multivibrator grids. The multivibrator is reset manually and the neon lamp is then illuminated. Any

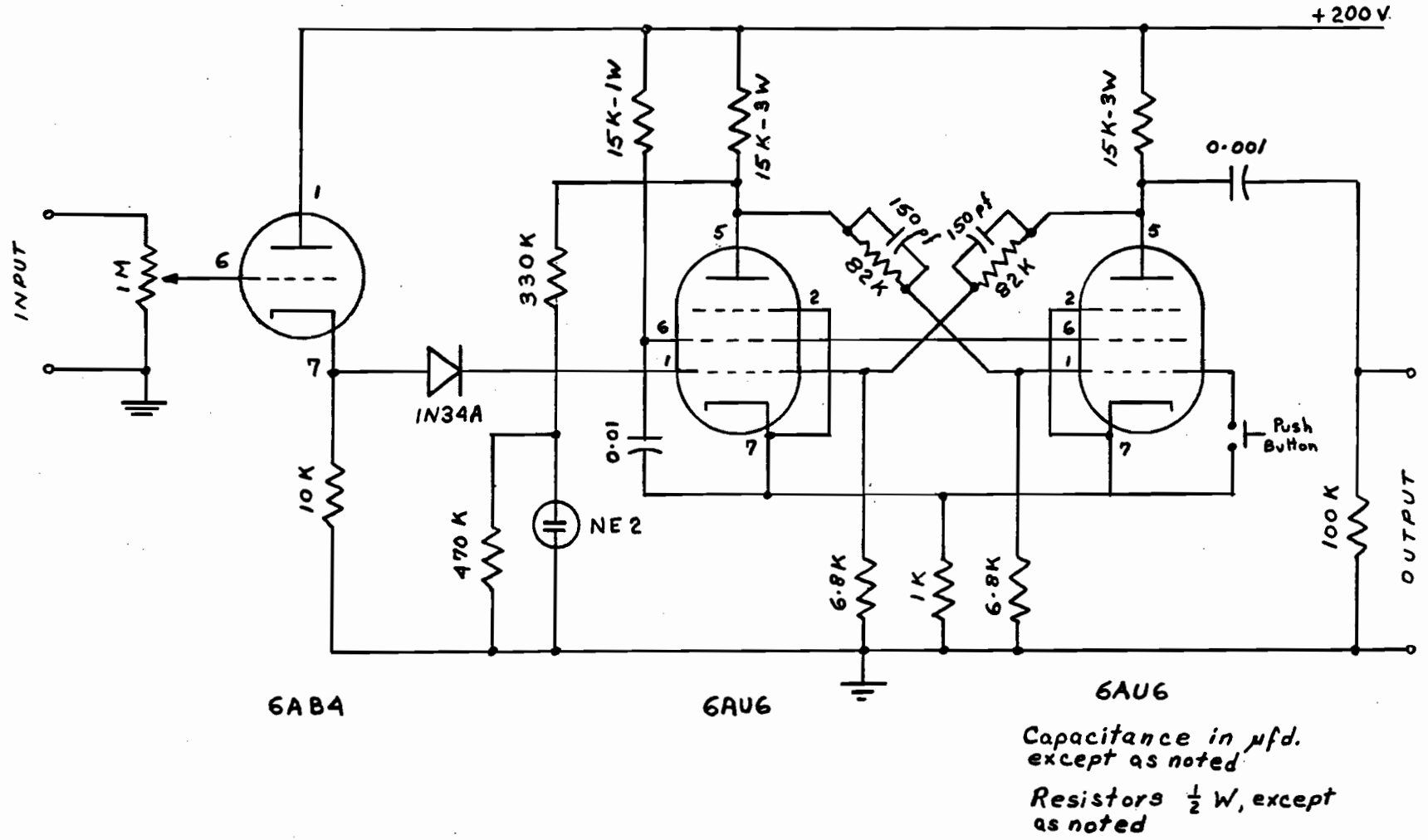

Figure 3.17

Bistable Multivibrator for Photographs

input signal which exceeds 8 volts will then cause the multivibrator to change states, producing a large pulse at the output terminals for triggering the sweep on a Type 502 oscilloscope. An input signal will not produce an output unless the push-button is first depressed. The setting of the input potentiometer is quite critical and must be readjusted if the input signal level is changed.

The trigger generator shown in Figure 3.4 is sometimes used when it is desired to use a point on the input signal waveform as a reference. Its circuit is shown in Figure 3.18 and it is comprised of a Schmidt Trigger[36] and a bistable multivibrator. Alternate positive and negative pulses appear at the output every time the input signal level equals 2 volts and has a negative slope. The upper frequency limit of this trigger is about 5 Kc.

The circuitry described above forms the basis of a flexible system for studying sampled-data circuits. The performance of these units is compared with theoretically predicted results in the next chapter.

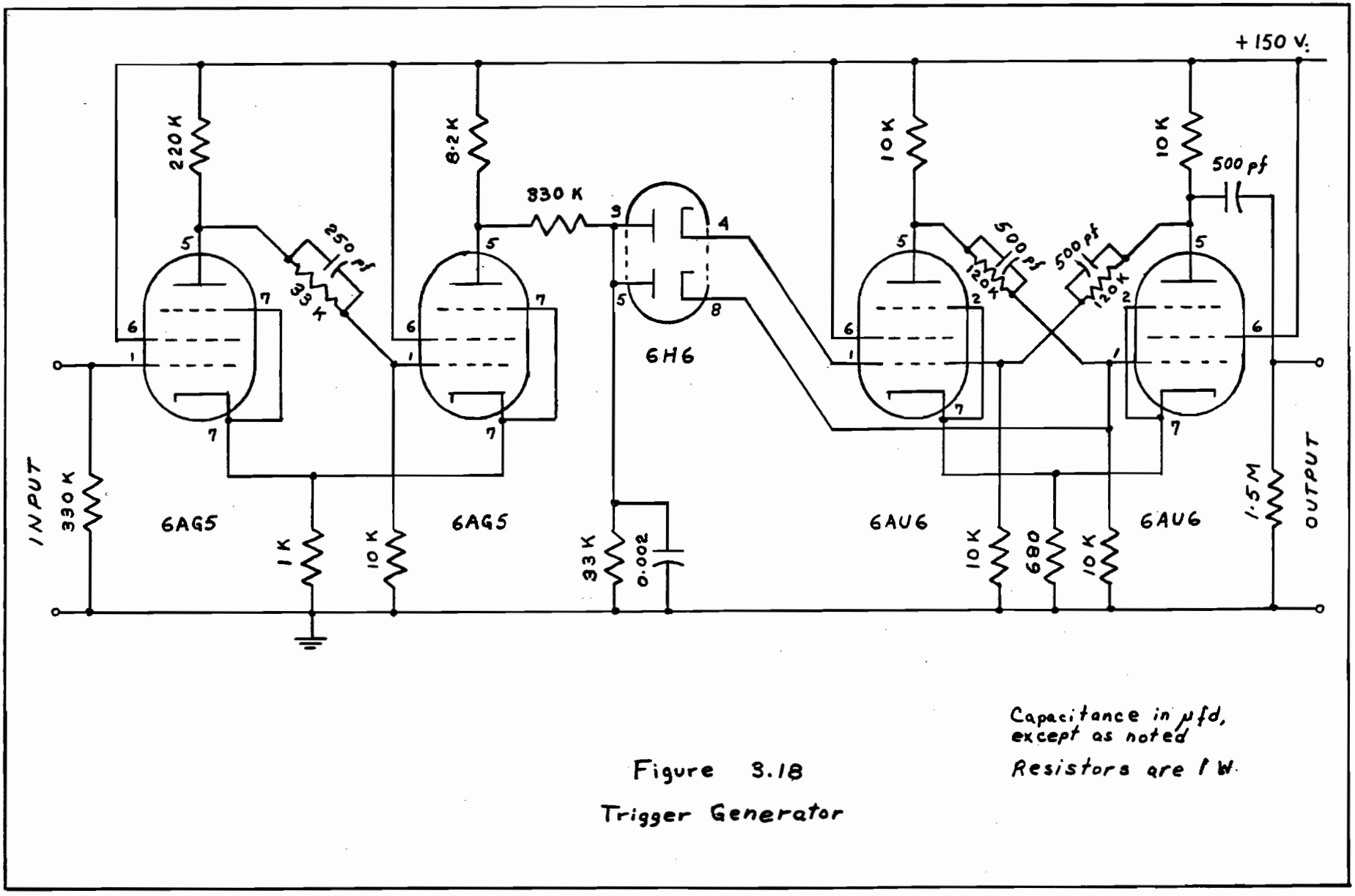

Capacitance in μfd, except as noted

Resistors are 1 W.

Figure 3.18

Trigger Generator

CHAPTER IV

THE EXPERIMENTAL PERFORMANCE OF A ZERO-ORDER HOLD

4.1 The Experimental Memory Unit.

The performance of the suggested circuit for simulating a memory storage element was evaluated by using this circuit as a zero-order hold. The component values used in the memory unit are shown in Figure 4.1.

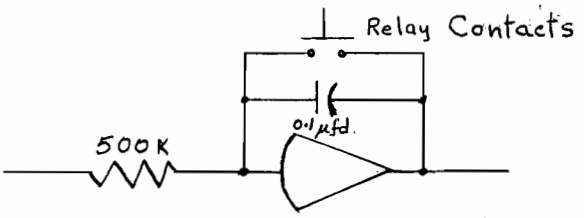

Figure 4.1

The experimental memory unit.

If the sampling pulse width is h msec., then the final value of the output of the integrator in Figure 4.1 is - 20 Ah mvolts, where Ah is the area of the pulse sample in millivolt-seconds. A typical input sample to the memory unit is shown in Figure 4.2a and the corresponding integrator output is illustrated in Figure 4.2b.

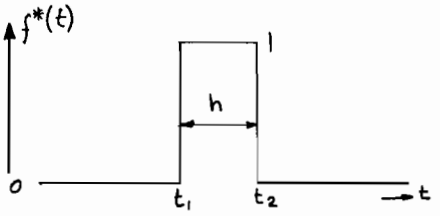

Figure 4.2a

A typical sample input.

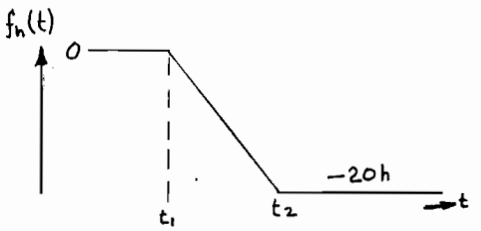

Figure 4.2b

Memory unit output.

The output from the experimental hold circuit is illustrated in Figures 4.3a and 4.3b. In the former, a 0.5 cps sine wave was sampled with 5 msec. pulses every 0.1 sec., and in the latter, a 2 cps sine wave was sampled with the same pulse train. The lower traces show the zero-order hold output, after inversion, and the detail of the interval between successive "steps" is similar to that shown in Figure 3.15. The slight slope of the "step runs" is due to the combined D-C unbalance of the operational amplifiers and the sampler output.

Because the input to the hold circuit is not an ideal impulse, the transfer function of the memory unit, M(s), should be written:

$$M(s) = \frac{1}{s} - \frac{h\, e^{-sT}}{1 - e^{-sh}} \qquad \ldots\ 4.1$$

where h is the width of the sampling pulses, and T is the sampling interval. When $h \ll T$ this may be replaced by the approximate, but more usual expression $M(s) = s^{-1}(1 - e^{-sT})$.

When the sampling pulse width is small, but the operational delay, δT, of the relay contacts discussed in Section 3.5 is comparable to the sampling interval, the transfer function of the memory unit is

$$M(s) = s^{-1}\,(1 - e^{-\mu sT}) \qquad \ldots\ 4.2$$

where $\mu = 1-\delta$. Because μ is not an integer, the term $e^{-\mu sT}$ may not be removed as a factor $z^{-\mu}$, as was done for the ideal hold circuit. If the modified Z-transform for the plant which follows the hold circuit is re-interpreted, however, a simple expression for the overall transfer function is obtained.

The modified Z-transform was derived by introducing a fictitious delay, ΔT, in the system output. However, the term $e^{-\mu sT}$ is

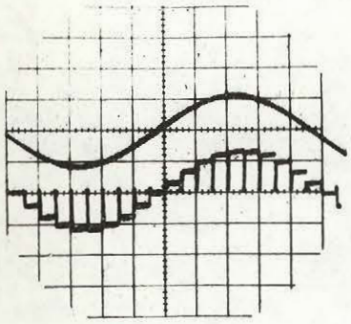

Figure 4.3a

Zero-order hold output with
20 samples/cycle

Input: 0.5 cps sine wave
Pulse Width: 5 msec
Pulse Spacing: 0.1 sec

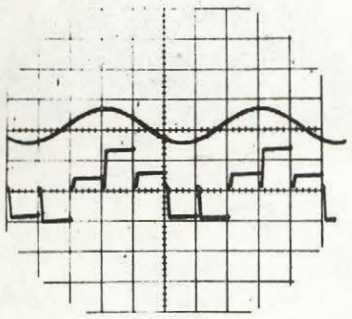

Figure 4.3b

Zero-order hold output with
5 samples/cycle

Input: 2 cps sine wave
Pulse Width: 5 msec
Pulse Spacing: 0.1 sec

equivalent to a real delay, μT, in the system. If we assume that ΔT includes both the fictitious delay, $\Delta' T$, and the real delay, μT, then $m = 1+\Delta = 1-\Delta'-\mu = \delta-\Delta'$, where δ is the delay introduced by the relay. Hence, in the modified Z-transform we should be using $m' = 1-\Delta'$, while we are actually using $m = \delta-\Delta'$. Therefore, we may write the modified Z-transform of the combined plant and hold circuit directly:

$$Z_m[T(s)] = Z_m[H'(s)] - Z_m[e^{-\mu sT} H'(s)] \quad \ldots. 4.3a$$

$$= H'(z,m) - H'(z,m') \quad \ldots. 4.3b$$

where $T(s)$ is the transfer function of the combined plant and hold circuit,

$H(s)$ is the transfer function of the plant alone,

and $H'(s) = H(s)/s$.

When the inverse transform is evaluated, $t = (n+m-1)T$ is used in the first term of equation 4.3b, and $t = (n+m'-1)T = (n+m-\delta)T$ is used in the second term. Thus the effect of the relay delay is included in inverse modified Z-transform and may be separated by appropriate interpretation.

A practical remark should be made concerning the use of these experimental hold circuits. This applies to the relative positioning of scaling amplifiers and integrators to minimize line frequency hum in the hold output. Consider the two arrangements shown in Figures 4.4a and 4.4b.

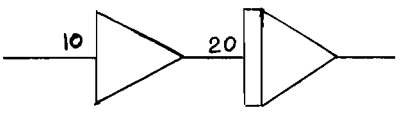

Figure 4.4a

Scaler precedes integrator.

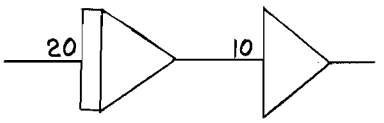

Figure 4.4b

Integrator precedes scaler.

If the hum, referred to the input of an operational amplifier, is x mv., then the hum in the output of configuration 4.4a will be $20(10x + x)/\omega$,

and in the other configuration it will be $10(20x/\omega + x)$, where ω is the angular frequency of the hum. For 60-cycle hum, these two expressions are approximately $x/2$ and $10x$. With the operational amplifiers in the Donner computer, $x = 10$ mv. peak-to-peak, and the hum output with configuration 4.4a was measured as 4 mv p-p, and with the other configuration as 110 mv p-p.

4.2 The Discontinuous Impulse Response of a Sampled-Data System.

The experimental study of a sampled-data system whose plant has a discontinuous impulse response, illustrates many of the features already discussed. The plant used was a resistor-capacitor integrating network, and the output was observed on the Moseley Model 2D recorder. The input impedance of the recorder is 2 megohms on the ranges used, shunted by a negligible capacitance. The equivalent circuit of the plant is shown in Figure 4.5. Its transfer function is $1/(2s+2)$, and has a discontinuous response as defined by equation 1.30.

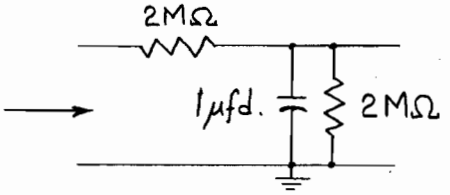

Figure 4.5

Equivalent circuit of experimental plant.

The modified Z-transform for the output of this plant, with a sampled unit step input is

$$O(z,m) = \frac{1}{2}\,\frac{z}{z-1}\,\frac{e^{-mT}}{z-e^{-T}} \qquad \ldots\ 4.4$$

where $O(z,m)$ is the modified Z-transform of the input to the recorder

T is the sampling interval.

The inverse Z-transform of equation 4.4 is

$$o(t) = \frac{e^{-mT}}{2} \frac{1-e^{-nT}}{1-e^{-T}} \qquad \ldots. 4.5$$

where $t = (n+m-1)T$.

o(t) in equation 4.5 is compared with the experimental output in Figure 4.6 for a sampling interval of 2.5 sec and a sampling pulse width of 50 msec. In this, and succeeding figures, the necessary scaling factors have been included in the theoretical points, which have also been shifted horizontally, when it was necessary to compensate for the uneven pulse spacing. The experimental curve shows a continuous impulse response, while equation 4.5 predicts finite discontinuities at the sampling instants. This experimental behaviour is partly due to the finite pulse width, but it is principally a manifestation of the recorder characteristics. The maximum writing speed of the Model 2D is 20 in/sec, so the recorder servomechanism behaves as a low-pass filter. Thus the overall plant, consisting of the integrator network, recorder input impedance, and the recorder servomechanism has a continuous impulse response, a point which must be noted in the experimental study of these systems.

When the pulse width is comparable to the sampling interval, the P-transform analysis must be used. In this case, the plant output for a sampled unit step input is given by the relation:

$$O(s) = \frac{1}{2} \frac{1-e^{-hs}}{s(1-e^{-sT})} \frac{1}{s+1} \qquad \ldots. 4.6$$

where O(s) is the Laplace transform of the input to the recorder

h is the sampling pulse width in seconds

T is the sampling interval in seconds.

The inverse P-transform of equation 4.6 is

$$o(t) = \left[1-d(-h)\right]\left\{ n - \frac{e^{-T(m-1)}-e^{-t}}{e^{T}-1} \right\} \qquad \ldots. \; 4.7$$

where $t = (n+m-1)T$.

$d(-h)$ is an operator introduced by Farmanfarma which denotes a delay of h seconds along the positive time axis.

$o(t)$ in equation 4.7 is compared with the experimental results in Figure 4.7 for a sampling interval of 2.5 sec and a pulse width of 0.5 sec. In this case the time-response of the recorder servomechanism is negligible compared to the sampling pulse width and the agreement between theory and experiment is quite good.

The discrepancies which do arise between theory and experiment are due to the usual sources, such as measuring the time intervals, scaling factors, sample heights and time constants accurately. Variations in the sampling interval times and non-linearities in the x-axis recorder servomechanism produce a record with uneven sample spacing.

4.3 The Response of a Sampled Data System Employing a Zero-Order Hold.

The performance of the circuit in Figure 4.1 was investigated by using it as the restoring element in the sampled-data system described in the preceding section. For the sampling intervals used, the delay due to the relay may be ignored, and the modified Z-transform of the recorder input is

$$O(z,m) = \frac{1}{2}\,\frac{z}{z-1}\,\frac{z-1}{z}\left\{ \frac{1}{z-1} - \frac{e^{-mT}}{z-e^{-T}} \right\} \qquad \ldots. \; 4.8$$

where $O(z,m)$ is the modified Z-transform of the recorder input for the combined plant and hold circuit.

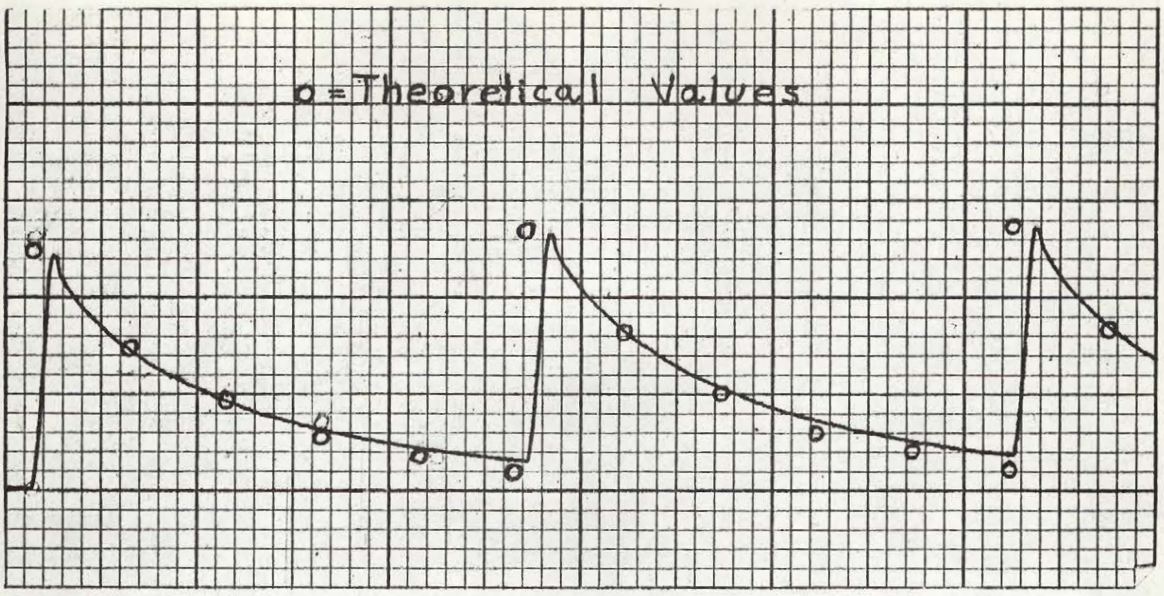

Figure 4.6

Output of a plant with a discontinuous impulse response when the sampling pulses are narrow.

Vert. Scale: 1 volt/inch
Horiz. Scale: 1 sec./inch

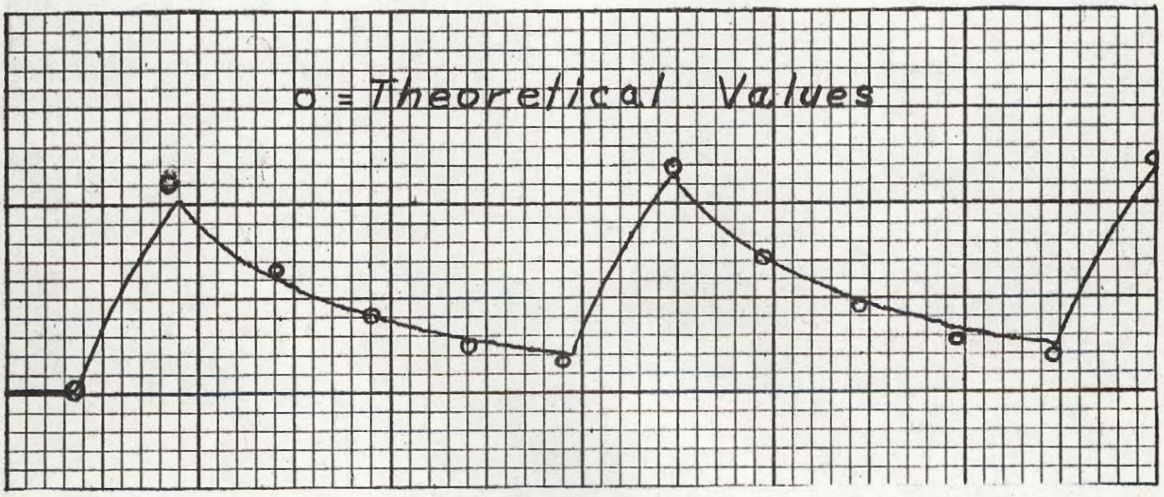

Figure 4.7

Output of a plant with a discontinuous impulse response when the sampling pulses are wide.

Vert. Scale: 5 volts/inch
Horiz. Scale: 1 sec./inch

The inverse transform of equation 4.8 is

$$o(t) = (1-e^{-(n+m-1)T})/2 \quad \ldots\ 4.9a$$

which, with the substitution $t = (n+m-1)T$ becomes

$$o(t) = (1-e^{-t})/2 \quad \ldots\ 4.9b$$

This is the same response which would be obtained if the unit step were applied directly to the plant, without the intervening sampling and restoration. Equation 4.9b is compared with the experimental results in Figure 4.8 for a sampling interval of 2.5 sec and a pulse width of 50 msec. The dips at the sampling instants are caused by the finite pulse width. It would appear that the time constant of the plant is slightly greater than 1 second.

When the sampling pulse width is comparable to the sampling interval, equation 4.1 must be used for the transfer function of the hold circuit. The Laplace transform of the recorder input is then

$$O(s) = \frac{1 - e^{-hs}}{s(1-e^{-sT})}\left\{\frac{1}{s} - \frac{h\, e^{-sT}}{1-e^{-sT}}\right\}\frac{1}{s+1} \quad \ldots\ 4.10$$

and the inverse P-transform of this relation is

$$o(t) = \left[1-d(-h)\right]\left\{\frac{n}{2}(mT+t) - n + \frac{e^{-T(m-1)} - e^{-t}}{e^{T} - 1}\right\} + h\left\{\frac{e^{-mT} - e^{-t}}{1 - e^{-T}} - n + 1\right\} \quad 4.11$$

Where $t = (n+m-1)T$, and the other symbols have their usual significance.

Equation 4.11 and the experimental results are compared in Figure 4.9 for a sampling interval of 2.5 sec and a pulse width of 0.5 sec. The dips are predicted by the P-transform analysis and are due to the finite pulse width.

These results show that the experimental memory circuit behaves as an ideal zero-order hold when the pulse width is small and the relay

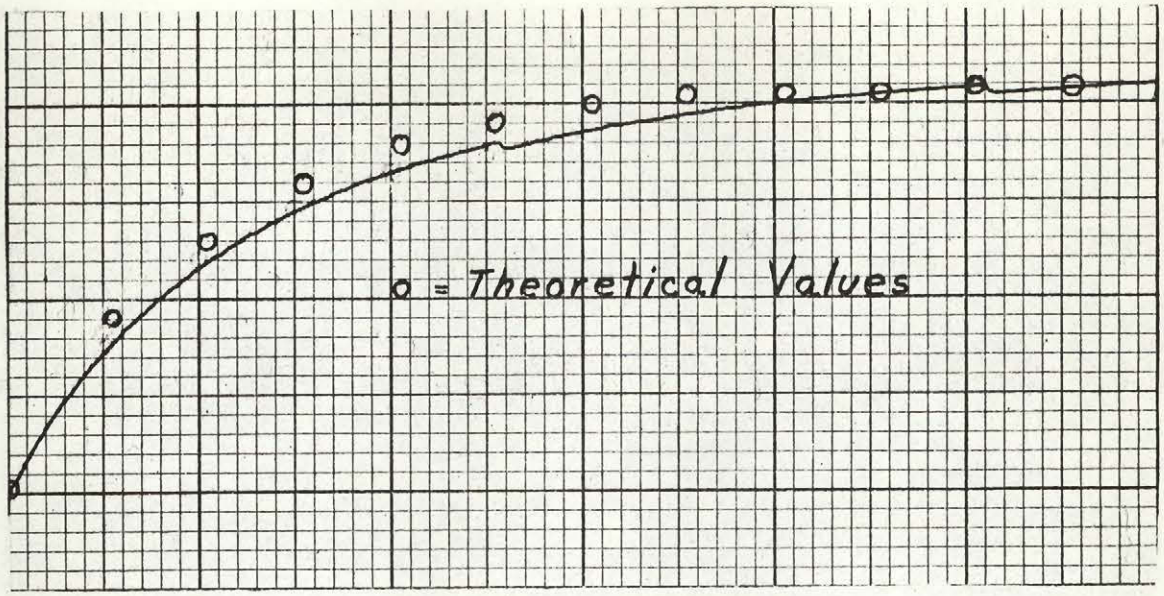

Figure 4.8

Output of a sampled-data system employing a hold circuit when the sampling pulses are narrow.

Vert. Scale: 1 volt/inch
Horiz. Scale: 1 sec./inch

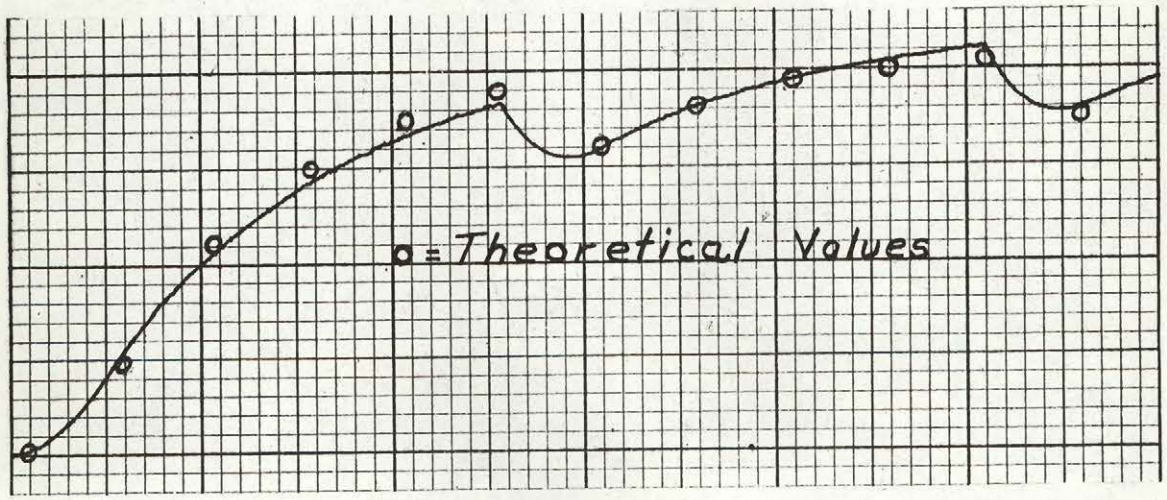

Figure 4.9

Output of a sampled-data system employing a hold circuit when the sampling pulses are wide.

Vert. Scale: 2 volts/inch
Horiz. Scale: 1 sec./inch

delay is negligible. When the pulse width is large, its performance is no longer that of the ideal hold, but, nevertheless, may be predicted by the P-transform analysis. However, if the memory unit is disconnected from the following circuit until the end of the sampling pulse, equation 4.3b may be used to predict its performance with δ equal to the combined delay of the relay and pulse width.

4.4 On Restoring Sampled Square Waves.

When the continuous input to the sampler is a square wave, it is possible, under certain conditions, to restore this waveform completely using a zero-order hold. This may be seen to be obvious, physically, by considering the time-domain sampling picture. If the sampling pulses occur at the start of every half cycle, then the hold output will consist of alternate positive and negative pulses with a duration equal to the sampling interval. This is the original square wave except for an amplitude scaling factor. Frequency-domain considerations indicate that although complementary frequency components are produced, these will coincide with the primary frequencies if the square wave period is an even multiple of the sampling interval.

These considerations may be established mathematically by analysing the square wave whose first cycle is shown in Figure 4.10.

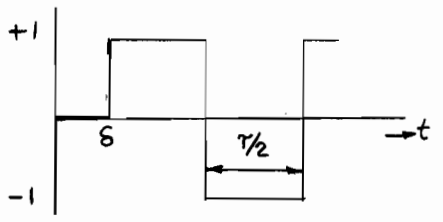

Figure 4.10

First cycle of the square wave input.

The delay, δ, is introduced for mathematical convenience, and will be allowed to go to 0 in the final expression. Physically, this means that the sampling pulses coinciding with each half-cycle of the square wave sample the wave to the left of the axis crossing. The Laplace transform of this square wave is

$$F(s) = \frac{1}{s} \frac{e^{\frac{s\tau}{2}} - 1}{e^{\frac{s\tau}{2}} + 1} e^{-\delta s} \qquad \ldots. \quad 4.12$$

where τ is the period of the square wave. Because $f(0^+) = 0$, we may use Linvill's expression (equation 1.4) for the Laplace transform of the sampled wave, which is

$$F^*(s) = \frac{1}{T_1} \sum_{k=-\infty}^{\infty} F(s + jk\omega_1) \qquad \ldots. \quad 4.13a$$

$$= \frac{1}{T_1} \sum_{k=-\infty}^{\infty} \frac{e^{\frac{jk\omega_1\tau}{2}} e^{\frac{s\tau}{2}} - 1}{e^{\frac{jk\omega_1\tau}{2}} e^{\frac{s\tau}{2}} + 1} \cdot \frac{e^{-\delta s} e^{-jk\delta\omega_1}}{s + jk\omega_1} \qquad \ldots. \quad 4.13b$$

where $T_1 = 2\pi/\omega_1$ is the sampling interval. As we want $F^*(s)$ to have the same general form as $F(s)$, we must have $\omega_1\tau/2 = 2n\pi$, where n is an integer. Physically, this means that the complementary frequency components must be coincident in the power spectrum with the primary components. With this substitution, equation 4.13b becomes

$$F^*(s) = \frac{e^{\frac{s\tau}{2}} - 1}{e^{\frac{s\tau}{2}} + 1} e^{-\delta s} \frac{1}{T_1} \sum_{k=-\infty}^{\infty} \frac{e^{-jk\delta\omega_1}}{s + jk\omega_1} \qquad \ldots. \quad 4.14$$

The summation may be written as

$$\frac{1}{T_1} \sum_{k=-\infty}^{\infty} \frac{e^{-jk\delta\omega_1}}{s + jk\omega_1} = \frac{1}{sT_1} + \frac{2}{T_1} \sum_{k=1}^{\infty} \frac{s\cos(x\delta) - x\sin(x\delta)}{s^2 + x^2} \qquad 4.15$$

where $x = 2\pi k/T_1$. With the aid of the summation properties of the modified Z-transform, the sum on the right-hand side of 4.15 may be

written[17]

$$\frac{1}{sT_1} + \frac{2}{T_1}\sum_{k=1}^{\infty} \frac{s\cos(x\delta) - x\sin(x\delta)}{s^2 + x^2} = \frac{e^{-sT_1(1-m)}}{1 - e^{-sT_1}} \quad \ldots\ 4.16$$

where $m<1$, and is defined by $\delta/T_1 = p+m$, where p is an integer. Thus, expression 4.14 becomes

$$F^*(s) = \frac{e^{\frac{sT}{2}} - 1}{e^{\frac{sT}{2}} + 1}\ e^{-pT_1 s}\ e^{-mT_1 s}\ \frac{e^{-sT_1(1-m)}}{1 - e^{-sT_1}} \quad \ldots\ 4.17a$$

$$= \frac{e^{\frac{sT}{2}} - 1}{e^{\frac{sT}{2}} + 1}\ \frac{e^{-sT_1(p+1)}}{1 - e^{-sT_1}} \quad \ldots\ 4.17b$$

The Laplace transform for a zero order hold is $s^{-1}(1-e^{-sT_1})$, multiplying 4.17b by this expression, we have

$$F_h(s) = \frac{e^{\frac{sT}{2}} - 1}{e^{\frac{sT}{2}} + 1}\ \frac{1}{s}\ e^{-sT_1(p+1)} \quad \ldots\ 4.18$$

where $F_h(s)$ is the Laplace transform of the hold output. Equation 4.18 states that the hold output will be a square wave delayed by p+1 sampling intervals. If $\delta \to 0$, then $p \to 0$, and the square wave from the hold circuit is delayed only one sampling interval. If the sampling pulses occurred to the right of the axis crossing, there would be no delay for $\delta = 0$.

This theory was tested by sampling and restoring a 5 cps square wave, using a sampling interval of 0.1 sec and a pulse width of 5 msec. The results are shown in Figure 4.11. The lower trace is the input, and the upper is the hold output. The inversion of the output is characteristic of the operational amplifier, and the delay occurs because the sampling pulses and input signal were not phase-synchronized. The slope of the leading edge of the restored wave is characteristic of the experimental hold operation.

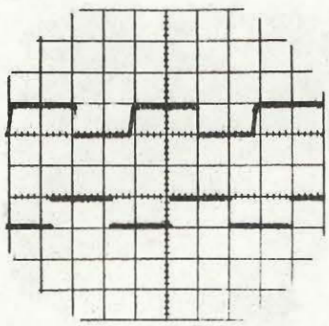

Figure 4.11

Restoration of a sampled square wave

The lower trace is the original 5 cps square wave. The restored output is shown in the upper trace. The sampling rate was 10 samples/sec with a pulse width of 5 msec. The inversion of the output is characteristic of operational amplifiers.

Although it has been demonstrated theoretically and experimentally that it is possible to restore a square wave completely by sampling at only twice its lowest frequency component, this does not pose any philosophical difficulties, since all the information in a square wave is known when its amplitude and time of axis crossings are specified, and this information is contained in the sampling pulse train.

4.5 Hold Circuit Frequency Response and Correlation Analysis.

So far, only the Z-transform and P-transform analysis of hold circuits has been considered, but it is also possible to study these as low-pass filters by considering their frequency response. The frequency response of a hold circuit may be obtained by substituting $s = j\omega$ in its transfer function (equation 2.41), and evaluating the amplitude and phase of the resulting expression. It is therefore desirable to have a laboratory technique for studying these quantities. Because of the low frequencies at which hold circuits are used, standard frequency analysers are not suitable, so this study is made with the aid of a digital computer.

The auto-correlation function, $\phi_{11}(\tau)$, of a periodic signal, $f_1(t)$, is defined[37] as

$$\phi_{11}(\tau) = \frac{1}{T_1}\int_0^{T_1} f_1(t)\, f_1(t+\tau)\, dt \qquad \ldots\ 4.19$$

where T_1 is the period of $f_1(t)$. This quantity is related to the power spectrum, $\Phi(\omega)$, of $f_1(t)$ by the Fourier transform

$$\Phi_{11}(\omega) = \frac{1}{T_1}\int_0^{T_1} \phi_{11}(\tau)\, \cos(\omega\tau)\, d\tau \qquad \ldots\ 4.20$$

If a sinusoid is sampled and applied to a filter, the power spectrum

of the output will give the square of the magnitude of the filter transfer function at the primary and complementary spectrum frequencies.

The foregoing predictions are tested experimentally by the following procedure. The output of the filter is recorded on one channel of the Sandborn recorder, and points taken from this chart are used in a digital computer auto-correlation program. The output of the auto-correlation program is the data cards for a Fourier cosine-transform program.

Enough data points must be tabulated for each cycle of the recorded waveform to ensure that the complementary frequency components, introduced by this sampling operation, do not affect the accuracy of the final computation. The programs which have been written are suitable for periodic signals, and their FORTRAN language statements for the IBM 650 computer will be found in Appendix III. In general, the power spectrum output will have a graph similar to Figure 4.12, and the power at a given frequency is then determined by taking the average height of the peak at this frequency. If the period of the filter output has been divided into an integral number of intervals in recording the data points, these peaks will become very sharp, and their average value may be determined by inspection of the computer output.

The final results obtained from the computer program were compared with predictions based on the known frequency response of the circuit. For the filters considered in this study, their frequency response is well known, and the comparison is a measure of the accuracy of the digital computer calculation.

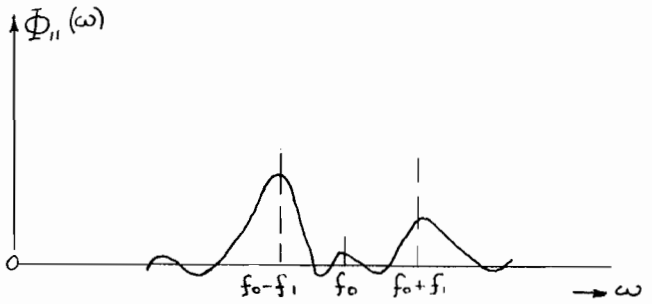

Figure 4.12

Typical power spectrum output.

The computer programs were tested by using them to measure the magnitude of the transfer function of the Krohn-Hite Model 330-A band-pass filter. This unit has a transfer function of the form $1/s^4$, and hence has a continuous impulse response. Figure 4.13 shows the Sandborn chart which was obtained when a 1 cps sine wave was sampled every 0.1 sec with a pulse width of 5 msec. The high and low cut-off frequencies of the filter were 5 cps and 0.02 cps, respectively. Data points were taken every millimeter (20 msec) of the record. The upper curve is the filter output and the lower is the original sine wave. The theoretical and experimental results are compared in Table 4.1.

Table 4.1

Comparison of computer-calculated, through 4.20, and directly measured low-pass filter frequency response.

Frequency	Relative Attentuation (db.)	
	calculated	measured
1 cps	0.0	0.0
9 cps	26	23
11 cps	31	29
19 cps	47	49

This experimental technique was also used to calculate the magnitude of the zero order hold transfer function, whose low-pass

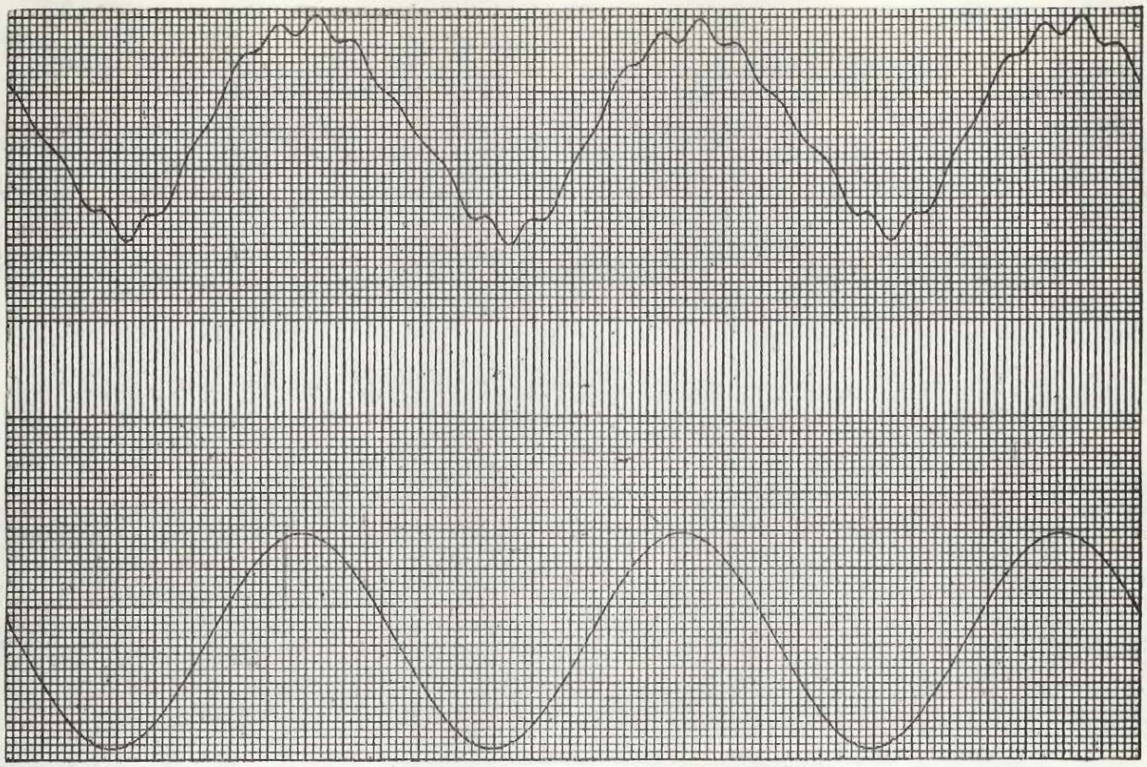

Figure 4.13

Two-channel recording of a sampled and filtered sine wave.

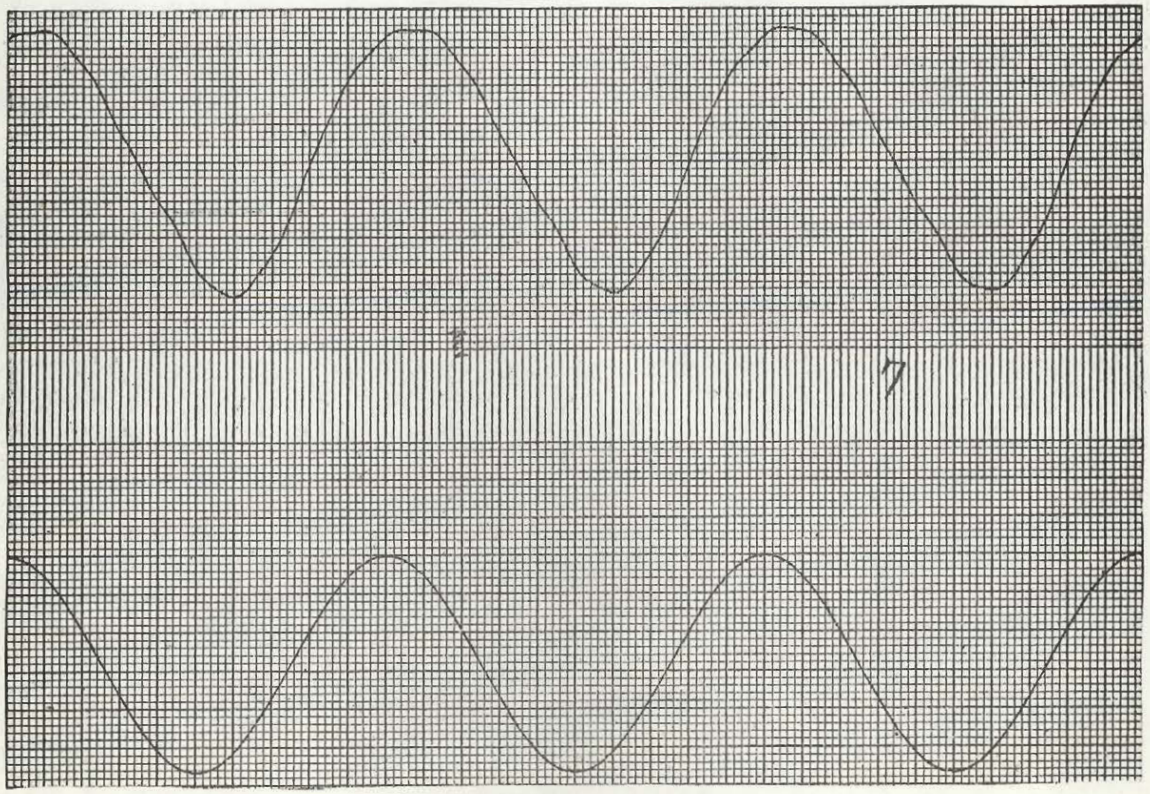

Figure 4.14

Recording of a sampled sine wave after (0,0) restoration and filtering.

characteristics are proportional to $(x^{-1}\sin x)^2$. For this study, it was postulated that 1 cps sine wave had been sampled at 10 cps and then restored. The resulting signal was easily calculated and 50 data points in each cycle were used in the computer auto-correlation program. The results of this computation are given in Table 4.2.

Table 4.2

Comparison of computer-calculated and theoretical zero order hold frequency response.

Frequency at which attenuation was determined.	Relative Attenuation (db.)	
	calculated on computer.	predicted from $(x^{-1}\sin x)^2$
1 cps	0.0	0.0
9 cps	18.6	19.2
11 cps	20.1	20.8
19 cps	23.5	24.5

The results in Tables 4.1 and 4.2 show that the power-spectrum calculation is a reasonably accurate method of measuring the magnitude of a filter transfer function at low frequencies. Nevertheless, there are many sources of error in this technique, one of which is the computer program itself. The accuracy of the final result is greatest if the waveform period is divided exactly into an integral number of intervals, as was done for the data in Table 4.2. For the data in Table 4.1, the values shown were determined by taking the area under the appropriate peaks, after the power spectrum was obtained. The precision with which values can be read on the Sandborn graph also affects the accuracy of the final figures. The curves in Figure 4.14 were obtained by using both zero-order hold restoration, and low-pass filtering, with the same input signal as for Figure 4.13. Although the

upper curve shows a greater restoration than that in Figure 4.13, it is not completely free of complementary frequencies. However, the calculated power spectrum values were so small as to indicate that the wave is monochromatic. A division of the waveform period into more intervals, and an improvement in the precision of the data points, would probably indicate otherwise.

CHAPTER V

CONCLUSIONS AND SUGGESTED FUTURE INVESTIGATIONS

5.1 Summary of the Results of this Research

A class of sampled-data filters, called the finite memory hold circuits, has been defined, and the Laplace transform for one group of these filter configurations has been evaluated, resulting in the definition of the H and P polynomials. One method of simulating these filters, using operational amplifiers, has been proposed and the feasibility of this method has been studied experimentally. A technique to measure the magnitude of the filter transfer function has also been suggested.

The experimental results indicate that operational amplifiers are quite suitable for the simulation of these hold circuits within the frequency range studied, although this is obviously only one of many possible methods. The performance of the experimental memory unit approximates the ideal when the sampling pulses are narrow. They may be predicted theoretically even when the sampling pulses are wide, or when the delay due to the feedback discharging cycle is appreciable.

Certain problems were encountered with the equipment which was used, such as drift and hum in the operational amplifiers. These are faults of the commercial units employed, however, and not deficiencies of the basic method.

5.2 Suggested Improvements in Laboratory Components and Experimental Techniques

The D-C unbalance in the sampler output can be reduced to a negligible value by using matched diodes for D_3 and D_4, a precision voltage divider in place of R_1 (Figure 3.7), and by replacing potentiometer R_2 by two matched Zener diodes. If there is no D-C unbalance in the sampler output, this basic circuit could replace the relay for discharging the integrator feedback capacitor, with a consequent reduction in the discharging cycle delay, and an increase in the flexibility of the simulation scheme. The sampler circuit can also be used to accomplish the necessary switching of the memory units, as outlined in Section 3.2.

A study of operational amplifiers, to determine the most suitable design for simulating the memory units, should be undertaken. Chopper stabilization is probably warranted, to reduce the D-C drift. Wide-band-width is necessary to ensure the accurate integration of very narrow pulses. The hum level must be reduced below that in the Donner Model 3000 amplifiers. These requirements may result in an operational amplifier of a design which is not available commercially. Alternatively, some system other than one employing operational amplifiers may be used, and the practical advantages of such systems must not be overlooked.

A more convenient method of obtaining data points for the auto-correlation program is also needed. Digital print-out devices have very low writing speeds, but it might be possible to sample the filter output at a high rate and record these samples on a magnetic tape for later measurement with a digital voltmeter. A better method would be to build an automatic auto-correlator, by using two samplers,

each controlled by identical but relatively-delayed pulse trains. After restoration by a (0,0) hold, the two signals would then be multiplied together electronically, and the product integrated for a suitable interval. The resulting signal would be recorded on the y-axis of an x-y plotter, while the x-axis of this plotter monitored a voltage proportional to the delay between the two pulse trains.

The auto-correlation method, although a powerful technique for determining the magnitude of a network transfer function, does not provide any information about the phase of this function. Phase information may be obtained by cross-correlation[37]. The complex Fourier transform of a system input-output cross-correlation function is the cross-power density spectrum of the input and output. When the latter quantity is divided by the density spectrum of the input signal, the magnitude and phase of the system transfer function is obtained. The cross-correlation function could be obtained automatically, using the device suggested above, if one of the two samplers monitors the filter input, while the other samples the output.

5.3 Possible Applications of the Finite Memory Hold Circuits

The finite memory hold circuits may be used as a digital to analog converter in a sampled-data system. Their use in conjunction with the analog computing scheme suggested by Hung[38] would result in a flexible laboratory computer which could perform most of the mathematical calculations of interest to electrical engineers, providing the solution in an analog form.

These sampled-data filters could also be used as function generators by pre-recording the necessary sample values on a magnetic tape, to generate a sufficiently accurate polynomial approximation to

the desired function. Complicated periodic functions could be generated by forming the magnetic tape into a loop.

Other workers[22, 23] have evaluated expressions for the optimum weighting functions of sampled-data filters to recover a sampled signal from noise. The finite memory hold circuit should also be tried in this application.

Sampled-data feedback systems are normally designed so they will not oscillate, but they may also be designed to oscillate at very low frequencies. The work of Franks and Sandberg[24] seems to indicate that such an oscillator, incorporating their N-path filter, would be very stable. The use of a finite memory hold circuit, rather than an N-path filter should be tried.

5.4 A Proposal for a Recognizing Machine

The invention of automatic computers has prompted researchers to "teach" these machines to perform some of the more complicated tasks which the human mind accomplishes so easily. Among these tasks is the recognition of an object under different lighting conditions, or of identical words when spoken by different individuals. The finite memory hold circuit promises to provide yet another method of building such a recognizing machine.

Consider the two words "we" and "me." When these are converted to an electrical signal, the initial transient is different in each case. Thus, it is their time-domain representation which seems to distinguish the two words. The finite memory hold circuit stores samples of the input signal in time sequence and is ideally suited for time-domain filtering in the sense described here.

To build this recognizing machine, tape recordings of identical words spoken by different individuals would be obtained. The electrical signals from these recordings would be sampled at a rate to be determined empirically, and these samples would be stored in the memory bank. The computing circuitry would be adjusted, not to restore these signals as accurately as possible, but to produce a unique output for a specific word. Such an adjustment should be made by the machine itself, by self-optimization of the filter transfer function.

This self-optimization would be accomplished by applying each of the recorded signals of the same word to the hold circuit, and "telling" the machine to produce the same output in all cases. By some suitable process the machine would adjust the sampling rate, amplifier gains and integrator time constants to obtain the desired result. Thus the machine would "learn" which parts of the signal are characteristic of a given word.

The final stage would be to obtain another set of recordings, this time of a different word, and to observe the filter output. If the outputs are unique and distinct from the output for the first word, the sampling rate, amplifier gains and integrator time constants would be recorded. From these figures the filter transfer function would be obtained and some information regarding the distinctive characteristics of words would be available to the researcher.

APPENDIX I

Properties of the H_m^r and P_m^r Polynomials

A1.1 - Definition of the Polynomials

The H_m^r polynomials are defined by:

$$H_m^r = \sum_{j=0}^{m-r} \frac{m!}{(m-j)!\,(Ts)^j} \qquad m>r \ .$$

$$= 1 \qquad m = r$$

$$= 0 \qquad m<r$$

The P_m^r polynomials are defined by:

$$P_m^r = H_{m+1}^{r+1} - H_m^r = \sum_{j=0}^{m-r} \frac{j!}{(m+1-j)!\,(Ts)^j}$$

A1.2 - Certain Recurrence Relations for these Polynomials.

$$H_m^r = 1 + (Ts)^{-1}\, m\, H_{m-1}^r \qquad \text{.... A1.1}$$

$$H_m^r - H_m^{r+1} = \frac{m!}{r!\,(Ts)^{m-r}} \qquad \text{.... A1.2}$$

$$H_{m+1}^r - H_m^r = (Ts)^{-1} H_m^r + (Ts)^{-1}\, m(H_m^r - H_{m-1}^r) \qquad \text{.... A1.3}$$

$$H_{m+1}^r - H_{m-1}^r = (Ts)^{-1}(m+1)H_m^r - (Ts)^{-1}(m-1)H_{m-2}^r \qquad \text{.... A1.4}$$

$$P_m^r = (Ts)^{-1} H_m^{r+1} + (Ts)^{-1} m\, P_{m-1}^r \qquad \text{.... A1.5}$$

$$P_m^r - P_m^{r+1} = \frac{(m-r)\,m!}{(r+1)!\,(Ts)^{m-r}} \qquad \text{.... A1.6}$$

$$P_m^r - P_{m-1}^r = \frac{(m-1)!}{r!(Ts)^{m-r}} + \frac{m+1}{Ts} P_{m-1}^r - \frac{m-1}{Ts} P_{m-2}^r \qquad \text{.... A1.7}$$

$$P_{m+1}^r - P_{m-1}^r = \frac{m+1}{Ts} P_m^r - \frac{m-1}{Ts} P_{m-2}^r + \frac{m+1}{(Ts)^2} H_m^r - \frac{m-1}{(Ts)^2} H_{m-2}^r \qquad \text{A1.8}$$

The above relations may be readily established from the definitions of the polynomials.

A1.3 - Values of Certain of these Polynomials

The first four H_m^o polynomials are:

$$H_o^o = 1 \qquad H_2^o = 1+2/Ts + 2/(Ts)^2$$

$$H_1^o = 1 + 1/Ts \qquad H_3^o = 1 + 3/Ts + 6/(Ts)^2 + 6/(Ts)^3$$

The first four H_m^1 polynomials are:

$$H_0^1 = 0 \qquad H_2^1 = 1 + 2/Ts$$

$$H_1^1 = 1 \qquad H_3^1 = 1 + 3/Ts + 6/(Ts)^2$$

The first four P_m^o polynomials are:

$$P_o^o = 0 \qquad P_2^o = 1/Ts + 4/(Ts)^2$$

$$P_1^o = 1/Ts \qquad P_3^o = 1/Ts + 6/(Ts)^2 + 18/(Ts)^3$$

These tables may be extended by use of the recursion formulae.

A1.4 - Modified Z-Transforms of H_m^r/s and P_m^r/s for the Values of H_m^r and P_m^r given in Section A1.3.

F(s)	F(z,m)	
H_o^o/s	$1/(z-1)$	A1.9
H_1^o/s	$\frac{m+1}{z-1} + \frac{1}{(z-1)^2}$	A1.10
H_2^o/s	$\frac{(m+1)^2}{z-1} + \frac{2m+3}{(z-1)^2} + \frac{2}{(z-1)^3}$	A1.11
H_3^o/s	$\frac{(m+1)^3}{z-1} + \frac{3m^2+9m+7}{(z-1)^2} + \frac{6m+12}{(z-1)^3} + \frac{6}{(z-1)^4}$	A1.12
H_o^1/s	0	A1.13

H_1^1/s $\qquad 1/(z-1)$ A1.14

H_2^1/s $\qquad \frac{2m+1}{z-1} + \frac{2}{(z-1)^2}$ A1.15

H_3^1/s $\qquad \frac{3m^2+3m+1}{z-1} + \frac{6m+6}{(z-1)^3} + \frac{6}{}$ A1.16

P_o^o/s $\qquad 0$ A1.17

P_1^o/s $\qquad \frac{m}{z-1} + \frac{1}{(z-1)^2}$ A1.18

P_2^o/s $\qquad \frac{2m^2+m}{z-1} + \frac{4m+3}{(z-1)^2} + \frac{4}{(z-1)^3}$ A1.19

P_3^o $\qquad \frac{3m^3+3m^2+m}{z-1} + \frac{9m^2+15m+7}{(z-1)^2} + \frac{18m+24}{(z-1)^3}$

$\qquad + \frac{18}{(z-1)^4}$ A1.20

APPENDIX II

A SCHEME FOR THE DETERMINATION OF ANALOG COMPUTER CONNECTIONS FOR THE SIMULATION OF A GROUP I FINITE MEMORY HOLD CIRCUIT

A2.1.- Synthesis of the Analog Computer Connections.

Let the symbol M_r denote the memory unit which stores the sample $f\left[(n-r)T\right]$. The determination of the analog computer connections may be reduced to a mechanical operation by the following scheme:

1) Lay out a column of p+q+1 boxes to denote the memory units. Alternate outputs from this column (the memory bank), starting with M_1, are connected to inverters so that the first differences may be formed by the succeeding computing elements. If the order, p, of the hold circuit is even, p/2 inverters are required, if it is odd, (p-1)/2 inverters are required.

2) The inverter bank is followed by p-1 banks of integrators, whose time constants are all equal to 1 second. The first bank has p-1 integrators, and each succeeding bank one less integrator than the former. The outputs of the integrators in a given bank are connected two-by-two to the inputs of the integrators in the next bank. The output of the integrator in each bank which is the one nearest the M_o memory unit is tapped-off for later interconnections. A total of p(p-1)/2 integrators are required in this step.

3) Connect every second memory unit output to a common summer. Start the connections with M_o if p is odd, otherwise start with M_1. The scaling factors in the summer are adjusted in accordance with the method discussed in the following section, for the moment they are

denoted by the symbol $C^r_{p,q}$, where r is the memory unit subscript. Connect the output of the summer and the remaining memory units to the first of p cascaded integrators. The scaling factors for the summer output is unity, and for the remaining memory units it is $C^r_{p,q}$.

4) The integrator outputs which were tapped-off in Step 2 are now connected. Label the integrator banks from 1 to p-1, starting with the first bank after the inverters. Connect the outputs of the integrators in the odd-numbered banks to a common summer, using a scaling factor of unity for all inputs. Connect the output of this summer, the tapped-off outputs of the integrators in the even-numbered banks, the output of M_o, and the output of the last of the p cascaded integrators of Step 3, all to a common final summer. The filter output is that of the final summer. The scaling factors for all inputs to the final summer will normally be unity, unless some other scaling factor is desired.

5) The final design may be checked by verifying that the number of operational amplifiers in any path from the output of $M_o, M_2, M_4, ..$ to output of the filter is odd, and the number of amplifiers from the output of $M_1, M_3, M_5, ..$ in such a path is even.

This scheme is quite mechanical, requiring no ingenuity on the part of the designer, and so is suitable for programming into a digital computer[39].

A2.2 - Determination of the Summer Scaling Factors.

An examination of equations 2.40 and 2.41, shows that the last q+1 terms in the general expression for $G_{p,q}(s)$ are all powers of $T^{-p}(t-nT)^p$. These terms may be denoted by S, where

$$S = T^{-p}(t-nT)^p \sum_{j=0}^{q} R_j \, \delta_n^{p+j} \qquad \text{.... A2.1}$$

and $R_0 = 1$. Substituting 2.24 in A2.1:

$$S = T^{-p}(t-nT)^p \sum_{j=0}^{q} \sum_{r=0}^{p+j} R_j (-1)^r \binom{p+j}{r} f(n_r T) \qquad \text{....A2.2a}$$

$$= T^{-p}(t-nT)^p \sum_{r=0}^{p+1} (-1)^r f(n_r T) \sum_{j=0}^{q} R_j \binom{p+j}{r} \qquad \text{.... A2.2b}$$

The second summation determines the coefficients of the $f(n_r T)$ terms, which are the scaling factors for the memory unit outputs. Therefore, we can write:

$$C^r_{p,q} = \sum_{j=0}^{q} R_j \binom{p+j}{r} \qquad \text{.... A2.3}$$

If the R_j are all different, this sum is evaluated to determine the necessary scaling factors in the main computer. In the particular case where $R_j = R$ for all j, this expression may be further simplified. Setting $R_j = R$, expression A2.3 becomes:

$$C^r_{p,q} = R \sum_{j=0}^{q} \frac{(p+j)!}{(p+j-r)!\ r!} \qquad \text{.... A2.4a}$$

$$= \frac{R}{r!} \sum_{j=0}^{q} \frac{(p+j)!}{(p+j-r)!} \qquad \text{.... A2.4b}$$

This sum is readily identified as the sum of ascending factorials, evaluated by Kunz:[30]

$$\sum_{j=0}^{q} \frac{(p+j)!}{(p+j-r)!} = \frac{(p+j+1)!}{(p+j-r)!(r+1)} \Bigg|_{j=-1}^{j=q} \qquad \text{....A2.5a}$$

$$= \frac{1}{r+1}\left\{\frac{(p+q+1)!}{(p+q-r)!} - \frac{p!}{(p-r-1)!}\right\} \qquad \text{.... A2.5b}$$

Substituting A2.5b in A2.4b,

$$C^r_{p,q} = \frac{R}{(r+1)!}\left\{\frac{(p+q+1)!}{(p+q-r)!} - \frac{p!}{(p-r-1)!}\right\} \qquad \text{.... A2.6a}$$

$$= R\left[\binom{p+q+1}{r+1} - \binom{p}{r+1}\right] \qquad \text{.... A2.6b}$$

where $\binom{p}{r+1} = \dfrac{p!}{(p-r-1)!\ (r+1)!}$

Equation A2.6b is readily evaluated numerically, with the aid of a table of binomial coefficients.[31]

APPENDIX III

CORRELATION AND POWER SPECTRUM COMPUTER PROGRAMS

A3.1 The Correlation Program

The numerical formula used is

$$\phi_{11}(\tau) = \sum_{j=0}^{N} f_1(j\delta)\, f_1(j\delta+\tau)$$

where $\tau = n\delta$ (n an integer), δ = interval between data points.

The FORTRAN Language statement for the IBM 650 computer is:

```
      DIMENSION X(500), Y(500)
1     READ, CODE, T, M, N, J
      READ, (X(I), I=1,M)
      GO TO (2,3,2,3), J
2     DO 4 I=1,M
4     Y(I) = X(I)
      GO TO 5
3     READ, (Y(I), I=1,M)
5     MAX = N-1
      DT = MAX
      DS = DT * 0.75
      MO = N-2
      LT = M-N+1
      DO 6 L=1,LT
      K = L-1
      TK = T * FLOTF(K)
      COR = X(1)*Y(L) + X(N)*Y(N+K)
      COR = COR/2.0
      GO TO (7,7,8,8),J
7     DO 10 I=2, MAX
```

```
10  COR = COR + X(I)*Y(I+K)
    COR = COR/DT
    GO TO 30
8   DO 20 I=3, MO,2
20  COR = COR + X(I)*Y(I+K)
    COR = COR/2.0
    DO 21 I=2,MAX,2
21  COR = COR + X(I)*Y(I+K)
    COR = COR/DS
30  GO TO (40,45,40,45),J
40  IF(K) 50,50,55
50  DIV = COR
55  CORNM = COR/DIV
    GO TO 60
45  CORNM = 0.0
60  PUNCH, CODE, MAX, K, TK, COR, CORNM
6   CONTINUE
    GO TO 1
    END
```

This program will compute either auto- or cross-correlation functions, using the Trapezoidal rule for the summation if there are an odd number of intervals, and Simpson's rule if there are an even number of intervals.

The data cards are prepared in 7/card form. When a cross-correlation is performed, two such decks are required. These data cards are preceded by a 5-word starter card:

Word 1 — Code number

Word 2 — δ = interval between data points (sec.)

Word 3 — Total number of data points in each deck (≤ 500)

Word 4 — Number of data points to be used in each summation

Word 5 —
- 1 for auto-correlation } Trap. rule
- 2 for cross-correlation }
- 3 for auto-correlation } Simpson's rule
- 4 for cross-correlation }

The output of this program will have 6 words on each card:

Word 1 — Code number

Word 2 — Number of intervals used in each summation

Word 3 — Cardinal number of point in correlation function

Word 4 — Value of τ at which $\phi_{11}(\tau)$ is evaluated

Word 5 — Value of $\phi_{11}(\tau)$

Word 6 — 0.0 is cross-correlation is used

Value of $\phi_{11}(\tau)$, normalized with respect to $\phi_{11}(0)$

A3.2 The Power Spectrum Program

The numerical approximation used is

$$\Phi_{11}(\omega) = \sum_{j=0}^{N} \phi_{11}(j\delta) \cos(j\omega\delta)$$

where δ is the interval between the data points used in the auto-correlation program.

The FORTRAN Language statement for the IBM 650 computer is

```
      DIMENSION T(500), COR(500)
1     READ, FD, FM, FS, M,J
      DO 2 I=1,M
      READ, NUM, A, B, T(I), COR(I), S, V
```

```
2   CONTINUE
    NUM = NUM + 10*J
    N = M-1
    DT = N
    DS = DT*0.75
    MO = M-2
    F = FS
3   W = F*6.28318
    ARG = W*T(1)
    AR2 = W*T(M)
    PS = COR(1)*COSF(ARG) + COR(M)*COSF(AR2)
    PS = PS/2.0
    GO TO (4,6),J
4   DO 5 I=2,N
    ARG = W*T(I)
5   PS = PS + COR(I)*COSF(ARG)
    PS = PS/DT
    GO TO 10
6   DO 7 I=3, MO,2
    ARG = W*T(I)
7   PS = PS + COR(I)*COSF(ARG)
    PS = PS/2.0
    DO 8 I=2, N,2
    ARG = W*T(I)
8   PS = PS + COR(I)*COSF(ARG)
    PS = PS/DS
10  PUNCH, NUM, N, F, PS
    IF(FM-F) 1,1,11
```

```
   11 F = F + FD
      GO TO 3
      END
```

This program computes the power spectrum from the output cards of the auto-correlation program, using the Trapezoidal rule if there are an odd number of intervals, and Simpson's rule if there are an even number of intervals. The deck of auto-correlation cards is preceded by a 5-word starter card:

Word 1	Desired frequency increment in power spectrum values
Word 2	Maximum frequency for which the power spectrum is to be computed
Word 3	Minimum frequency for which the power spectrum is to be computed
Word 4	Total number of input cards
Word 5	1 for Trapezoidal rule 2 for Simpson's rule

The cards in the output deck have 4 words:

Word 1	Code number in auto-correlation program increased by 10 if Trapezoidal rule is used, increased by 20 is Simpson's rule is used
Word 2	Number of intervals used in the summation
Word 3	Frequency at which the power spectrum is evaluated
Word 4	Value of the power spectrum

BIBLIOGRAPHY

1. James, Nichols and Phillips, "Theory of Servomechanisms," Vol. 25, MIT Rad. Lab. Series, McGraw-Hill, New York (1947)

2. H. Freeman and O. Lowenchuss, "Bibliography of Sampled-data Control Systems and Z-Transform Applications," IRE Trans. on Automatic Control, No. PGAC-4, pp. 28-30, March 1958.

3. P. R. Stromer, "A Selective Bibliography on Sampled-data Systems," IRE Trans. on Automatic Control, No. PGAC-6, pp. 112-114, December 1958.

4. D. J. Gimpel, "Sampled-data Systems", Control Engineering, Vol.4, pp. 99-106, February 1957.

5. L. A. MacColl, "Fundamental Theory of Servomechanisms," (Book), pp. 88-101, Van Nostrand, New York (1945).

6. W. K. Linvill, "Sampled-data Control Systems Studied through Comparison of Sampling with Amplitude Modulation," Trans. AIEE, Vol. 70, pt. 2, pp. 1779-1788, 1951.

7. C. E. Shannon, "Communication in the Presence of Noise," Proc. IRE, Vol. 37, No. 1, pp. 10-21, 1949.

8. G. V. Lago, "Addition to Sampled-data Theory," Proc. Natl. Elec. Conf., Vol. 10, pp. 758-766, February 1955.

9. Bromwich, "Theory of Infinite Series," (Book), p. 318, No. 22, MacMillan.

10. J. R. Ragazzini and L. A. Zadeh, "The Analysis of Sampled-data Systems," Trans. AIEE, Vol. 71, Pt. 2, pp. 225-234, November 1952.

11. M. F. Gardner and J. L. Barnes, "Transients in Linear Systems, Vol. 1" (Book), Wiley, New York (1942).

12. E. I. Jury, "Analysis and Synthesis of Sampled-Data Control Systems" Trans. AIEE, Vol. 73, Pt. 1, pp. 332-346, 1954.

13. E. I. Jury, "Sampled Data Control Systems," (Book), Wiley, New York (1958).

14. D. K. Cheng, "Analysis of Linear Systems," (Book), Addison-Wesley, Reading, Mass. (1959).

15. R. H. Barker, "The Pulse Transfer Function and its Application to Sampling Servo Systems," Proc. IEE, Vol. 99, Pt. 4, pp. 302-317, 1952.

16. E. I. Jury, "Synthesis and Critical Study of Sampled-data Control Systems," Trans. AIEE, Vol. 75, Pt. 2, pp. 141-151, 1956.

17. E. I. Jury, "Additions to the Modified Z-transform Methods," 1957 IRE WESCON Conv. Record, Pt. 4, pp.136-156.

18. G. V. Lago, "Additions to Z-transformation Theory for Sampled-data Systems," Trans. AIEE, Vol. 73, Pt. 2, pp. 403-408, 1955.

19. G. Farmanfarma, "Analysis of Linear Sampled-data Systems with Finite Pulse Width (Open Loop)," Trans. AIEE, Vol. 75, Pt. 1, pp. 808-819, 1956.

20. G. Farmanfarma, "Analysis of Multiple-Sampler Systems with Finite Pulse Width (Open Loop)," Trans. AIEE, Vol. 77, Pt. 2, pp.20-28, 1958.

21. G. Farmanfarma, "General Analysis and Stability Study of Finite Pulsed Feedback Systems," Trans. AIEE, Vol. 77, Pt. 2, pp. 148-162, 1958.

22. H. C. Hsieh and C.T. Leondes, "On the Optimum Synthesis of Sampled-data Multipole Filters with Random and Non-Random Inputs," 1960 IRE Intnatl. Conv. Record, Pt. 4, pp. 37-52.

23. H. C. Hsieh, "On the Optimum Synthesis of Random Sampling Multipole Filters with Stationary Inputs," paper at AIEE Summer General Meeting, Cornell University, June 1961.

24. L. E. Franks and I. W. Sandberg, "An Alternative Approach to the Realization of Network Transfer Functions: The N-path Filter," BSTJ, Vol. 39, pp. 1321-1350, September 1960.

25. D. Gabor, W.P.L. Wilby and R. Woodcock, "A Universal Non-linear Filter, Predictor and Simulator which Optimizes itself by a Learning Process," Proc. IEE, Vol. 108, Pt. B, pp. 422-438, July 1961.

26. R. C. Klein, "Analog Simulation of Sampled-data Systems," IRE Trans. on Telemetry and Remote Control, Vol. TRC-1, pp. 2-7, May 1955.

27. R. C. Dorf and R. L. Enos, "An Analog Simulation of a Discrete Compensator for a Sampled-data System," paper at AIEE Summer General Meeting, Cornell University, June 1961.

28. A Porter and F. W. Stoneman, "A New Approach to the Design of Pulse-Monitored Servo Systems," Proc. IEE, Vol. 97, Pt. 2, pp. 597-610, 1950.

29. P. F. Lawden, "A General Theory of Sampling Servo Systems," Proc. IEE, Vol. 98, Pt. 4, pp.31-36, 1961.

30. K. S. Kunz, "Numerical Analysis," (Book), McGraw-Hill, New York, (1957).

31. H. B. Dwight, "Tables of Integrals and Other Mathematical Data," Second Edition, (Book), Macmillan, New York (1947).

32. G. A. Korn and T. M. Korn, "Electronic Analog Computers," (Book), McGraw-Hill, New York (1956).

33. F.E. Terman, "Radio Engineers' Handbook," (Book), McGraw-Hill, New York (1943).

34. DeWitt and Rossoff, "Transistor Electronics," (Book), McGraw-Hill, New York.

35. B. Chance, V. Hughes, E. F. MacNichol, D. Sayre and F. C. Williams, "Waveforms," Vol. 19, MIT Rad. Lab. Series, McGraw-Hill, New York (1949).

36. "Reference Data for Radio Engineers," Fourth Edition, (Book), International Telephone and Telegraph Corporation, New York (1959).

37. Y. W. Lee, "Statistical Theory of Communication," (Book), Wiley, New York (1960).

38. H. Hung, "A Sampled-data Differentiation Scheme on the Analog Computer," Master of Engineering Thesis, McGill University, August 1961.

39. C. R. Warburton, "Automation of Logic Page Pringing," paper at AIEE Summer General Meeting, Cornell University, June 1961.